Plant Physiology Preview. Published on August 27, 2019, as DOI:10.1104/pp.19.00591

Short Title: Looking Inside the Esca Symptomatic Leaf

Exploring the Hydraulic Failure Hypothesis of Esca Leaf Symptom Formation

Giovanni Bortolami, Gregory A. Gambetta, Sylvain Delzon, Laurent J. Lamarque, Jérôme Pouzoulet, Eric Badel, Régis Burlett, Guillaume Charrier, Hervé Cochard, Silvina Dayer, Steven Jansen, Andrew King, Pascal Lecomte, Frederic Lens, José M. Torres-Ruiz, Chloé E. L. Delmas*

SAVE, INRA, BSA, ISVV, 33882 Villenave d'Ornon, France (G.B., P.L., C.E.L.D.)
EGFV, Bordeaux-Sciences Agro, INRA, Univ. Bordeaux, ISVV, 210 chemin de Leysotte 33882 Villenave d'Ornon , France (G.A.G., J.P., S. Dayer)
BIOGECO, INRA, Univ. Bordeaux, 33610 Cestas, France (S. Delzon, L.J.L., R.B.)
Université Clermont Auvergne, INRA, PIAF, F-63000 Clermont-Ferrand, France (E.B., G.C., J.M.T.R., H.C.)
Institute of Systematic Botany and Ecology, Ulm University, D-89081 Ulm, Germany (S.J.)
Synchrotron SOLEIL, L'Orme de Merisiers, Saint Aubin-BP48, 91192 Gif-sur-Yvette cedex, France (A.K.)
Naturalis Biodiversity Center, Leiden University, P.O. Box 9517, 2300RA Leiden, The Netherlands (F.L.)
* Address correspondence to chloe.delmas@inra.fr
The author responsible for distribution of materials integral to the findings presented in this article in accordance with the policy described in the Instructions for Authors (www.plantphysiol.org) is: Chloé Delmas chloe.delmas@inra.fr.

One sentence summary: Leaf scorch symptom development is associated with the disruption of vessel integrity.

Author Contributions

C.E.L.D., G.A.G., G.B., and S. Delzon designed experiments and analysed the data; A.K., E.B., F.L., G.A.G., G.B., G.C., H.C., J.M.T.R., L.J.L., R.B., S. Dayer, S. Delzon, and S.J. participated in synchrotron campaigns; C.E.L.D. and G.B. conducted the histological observation; P.L. provided data on disease history of the plants used in this study; J.P. conducted the pathogen detection; G.B. analysed the micro CT images; C.E.L.D., G.A.G., and G.B. wrote the manuscript; All authors edited and agreed on the last version of the manuscript.

ABSTRACT

Vascular pathogens cause disease in a large spectrum of perennial plants, with leaf scorch being one of the most conspicuous symptoms. Esca in grapevine (*Vitis vinifera*) is a vascular disease with huge negative effects on grape yield and the wine industry. One prominent hypothesis suggests that vascular disease leaf scorch is caused by fungal pathogen-derived elicitors and toxins. Another hypothesis suggests that leaf scorch is caused by hydraulic failure due to air-embolism, the pathogen itself, and/or plant-derived tyloses and gels. In this study we transplanted mature, naturally infected esca symptomatic vines from the field into pots, allowing us to explore xylem integrity in leaves (*i.e.* leaf mid-veins and petioles) using synchrotron-based *in vivo* X-ray micro-computed tomography and light microscopy. Our results demonstrated that symptomatic leaves are not associated with air embolism. In contrast, symptomatic leaves presented significantly more non-functional vessels resulting from the presence of non-gaseous embolisms (i.e. tyloses and gels) than control leaves, but there was no significant correlation with disease severity. Using quantitative PCR, we determined that two vascular pathogen species associated with esca necrosis in the trunk were not found in leaves where occlusions were observed. Together these results demonstrate that symptom development is associated with the disruption of vessel integrity and suggest that symptoms are elicited at a distance from the trunk where fungal infections occur. These findings open new perspectives on esca symptom expression where the hydraulic failure and elicitor/toxin hypotheses are not necessarily mutually exclusive.

INTRODUCTION

Maintaining the integrity of the plant vascular system is crucial for plant health and productivity. Xylem tissue transports water and mineral nutrients and forms a complex reticulate network of many interconnected vessels (Zimmermann 1983). This complex network of vessels hosts a large breadth of endophytic microorganisms, most of which live harmlessly within the plant (Fisher et al. 1993; Oses et al. 2008; Qi et al. 2012, among others). However, some organisms in the vessel lumina can be (or become) pathogenic, and this class of pathogens is referred to as vascular pathogens (Pearce et al. 1996). Vascular pathogens are highly diverse, and their pathologies depend on the specific pathogen-host interaction. They cause diseases in a wide taxonomic range of plant species.

Plant vascular disorders are sometimes identified by conspicuous leaf scorch symptoms, which are strikingly similar and typically begin with necrosis at the leaf margin. The exact mechanisms driving these leaf symptoms remain largely unknown, and there are two long-standing and unresolved working hypotheses (Fradin and Thomma 2006; Surico et al. 2006; McElrone et al. 2010; Sun et al. 2013; Yadeta and Thomma 2013; Oliva et al. 2014; Pouzoulet et al. 2014). The first hypothesis proposes symptoms result from the transport of pathogen-derived elicitors or toxins through the transpiration stream. The second proposes symptoms result from hydraulic failure resulting from any combination of air embolism, occlusion of xylem vessels from the pathogen itself, and/or occlusion of xylem vessels by plant-derived tyloses and gels.

Esca disease in grapevine (*Vitis vinifera*) is one case where the conflict between these two hypotheses of leaf symptom formation remains unresolved (Surico 2006; Pouzoulet et al. 2014). Esca is characterized by three main symptoms: leaf scorch, trunk necrosis, and a colored stripe along the vasculature (Lecomte et al. 2012). Esca belongs to a complex of diseases referred to as grapevine trunk diseases (GTDs), which cause defoliation, berry loss, and vine death (Bertsch et al. 2013; Mondello et al. 2018). This disease has been recognized for thousands of years and has been increasingly the focus of research over the past two decades as it is believed to be one of the main causes of grape production decline, especially in Europe, USA (California), and South Africa (Cloete et al. 2015; Guerin-Dubrana et al. 2019). The fungi most strongly associated with esca wood necrosis in the trunk have been identified (Larignon and Dubos 1997; Mugnai et al. 1999; Fischer 2006; White et al. 2011;

Bruez et al. 2014, Morales-Cruz et al. 2018). While the disease was formerly associated with the presence of soft rot (caused by basidiomycetes such as *Fomitiporia mediterranea*), studies have identified two vascular pathogens, *Phaeomoniella chlamydospora* and *Phaeoacremonium minimum*, which are detected in trunk necrotic tissues of esca symptomatic vines (Feliciano et al. 2004; Massonnet et al. 2018; Morales-Cruz et al. 2018). Esca leaf symptoms are only observed on mature vines (>7 years-old) in the field (Mondello et al. 2018) and cannot be reliably reproduced by inoculating vines with the causal fungi (Surico et al. 2006, but see Bruno et al. 2007) despite testing various methodologies (Reis et al. 2019). This suggests leaf scorch symptoms are the result of complex host-pathogen-environment interactions (Fischer and Peighami Ashnaei 2019). Neither the elicitor/toxin nor the hydraulic failure hypothesis of esca pathogenesis has been experimentally confirmed. It is generally accepted that the fungi responsible for esca wood necrosis are not present in leaves and that leaf symptoms are a consequence of fungal activities in the perennial organs (i.e. trunk). However, to our knowledge, leaves and current-year stems have never been investigated in detail to see if the key pathogens detected in necrotic regions of the perennial wood also occur in these organs.

In the current study we created an experimental system for the study of esca disease by transplanting mature, naturally infected esca symptomatic vines from the field into large pots. This allowed us to test the hydraulic failure hypothesis by exploring vessel integrity (presence of air-embolism, occlusion, pathogens themselves) in leaves using non-invasive, *in vivo* imaging via X-ray micro-computed tomography (microCT), light microscopy, and qPCR. MicroCT avoids artifacts caused by traditional invasive techniques (Torres-Ruiz et al. 2015) and allows for the visualization of vessel content and functionality in esca symptomatic leaf petioles and midribs. We assessed the presence of two of the main pathogens associated with esca, *P. chlamydospora* and *P. minimum*, using qPCR in annual stems, leaves, and multi-year branches. These two species are tracheomycotic agents and could thus, in theory, disperse systemically via the sap flow from the trunk (Pouzoulet et al. 2014). This study provides new perspectives regarding the pathogenesis of esca leaf symptom formation.

RESULTS

Vessel Occlusion and the Percentage Loss of Conductivity in Symptomatic and Asymptomatic Leaves

Midrib and petiole vascular bundles of symptomatic and asymptomatic leaves were imaged in 3D using microCT (Figure 1; Supplemental Figures S1-S2). These analyses allowed for the identification of embolized and occluded xylem vessels and the quantification of the percentage loss of theoretical hydraulic conductivity (PLC). The level of native air embolism was very low, ranging from 2.8% to 9.7%, for both asymptomatic and symptomatic midribs (Figure 1 A,C) and petioles (Supplemental Figure S1 A,D). There were no significant differences in the levels of native air embolism between symptomatic and asymptomatic leaves in petioles or midribs (Table 1, Figure 2).

After exposing the xylem vessels to air by cutting the leaf or petiole just above (< 2mm) the scanned area, some proportion of vessels did not embolize immediately and apparently remained water-filled (Figure 1 B,D; Supplemental Figure S1 B,E red arrows; Supplemental Figure S2 C,D). These vessels were considered occluded. The average PLC in asymptomatic midribs due to occluded vessels was 12.4% (± 3.2), while symptomatic midribs showed significantly higher values, 68.8% (± 6.4) (Table 1, Figure 3). This is also the case for petioles where asymptomatic leaves exhibited a PLC of only 1.9% (± 1.8) while PLC in symptomatic leaves was 55.3% (± 9) (Table 1, Figure 3). Detailed information on the contributions of different kinds of vessels to the theoretical hydraulic conductivity are presented in Supplemental Table S1.

The Nature of the Xylem Vessel Occlusions

We investigated the nature of the vessel occlusions causing the high percentage of non-functional vessels in esca symptomatic leaves using microCT and light microscopy. MicroCT was conducted both with and without the contrasting agent iohexol, which has been utilized previously to track the transpiration pathway and determine vessel functionality (as described by Pratt and Jacobsen, 2018). The subsequent robust (examining >200 cross sections per microCT volume) and detailed (examining both cross and longitudinal sections) examinations of the microCT volumes in symptomatic leaves revealed that the nature of the vessel occlusions is complex (Figure 4). Occlusions can be larger, spanning the entire diameter of the vessel (Figure 4A, red arrows) or smaller occupying only a portion of the vessel (Figure 4A, yellow arrows). Longitudinal sections of iohexol-fed symptomatic leaves revealed the transpiration pathway can pass in between occlusions and through vessel connections (Figure 4A, white arrow) but never diffuse in surrounding tissues. In asymptomatic samples fed with

iohexol, occlusions expanding in iohexol-filled vessels were not observed (Supplemental Figure S3). Some partially-occluded vessels did not become air-filled upon cutting (compare Figures 4B with 4C) and occlusions were also visible (although they were more obscure) in entirely occluded, non-functional vessels that did not fill with air after cutting (Figure 4D, red arrows). When partially-occluded vessels embolized after cutting, occlusions were easily visualized (Figure 4E, red arrows). In these cases the contact angle between these occlusions and the vessel wall was quantified and was always higher than 100° with the highest frequency between 120° and 150° (Figure 4F). Partially-occluded vessels made up a small percentage of the total calculated PLC representing 8.1% ± 3.7 for symptomatic midribs and 1.3% ± 0.6 for symptomatic petioles, while in asymptomatic leaves partially-occluded vessels were never observed (Supplemental Table S1). A negligible percentage of partially-occluded vessels was observed within the native embolized vessels (i.e. air-filled prior to cutting the samples) corresponding to 0.3% ± 0.2 in symptomatic midribs and 0.4% ± 0.2 in symptomatic petioles (Supplemental Table S1).

The presence of these occlusions was likewise identified by light microscopy observations on symptomatic leaves (Figure 5). To identify the chemical nature of the occlusions, cross sections were stained with four different dyes: toluidine blue O (Figure 5A) in blue and periodic acid-Schiff's reaction (Figure 5B) in red indicate the presence of polysaccharides and polyphenols. Ruthenium red (Figure 5C) staining in pink for non- methyl-esterified pectins and lacmoid blue (Figure 5D) showing the presence of callose in grey-pink shades. Quantifying the number of occluded vessels in histology cross sections of midribs, we found an average of 19.7% (±11.6) of vessels with occlusions in symptomatic leaves, while just 0.4% (±0.1) of vessels contained occlusions in asymptomatic leaves (Supplemental Table S2, Supplemental Figure S4).

Relationship Between Leaf Symptoms and Occlusion

Leaf symptom severity, quantified by the percentage of green tissue (in pixels) of each leaf, ranged from 6.1% to 93.9% for symptomatic leaves. In asymptomatic leaves, green tissue always accounted for 100%. We found no significant relationship between the percentage of green tissue (*i.e.* symptom severity) and PLC due to occluded vessels in symptomatic leaves ($F_{1,17}$ = 1.43, *P*-value = 0.25; Figure 6). Additionally, there was no significant relationship

between percentage of green tissue and PLC when analyzed by plant or by organ ($F_{3,17}$ = 0.31, *P*-value = 0.81; $F_{1,17}$ = 0.80, *P*-value = 0.38, respectively).

Fungi Detection

The two vascular pathogens, *P. chlamydospora* and *P. minimum*, were not detected in leaves or lignified shoots. In 2-year-old cordons, their presence was detected in some samples but not others, regardless of whether the vines were symptomatic or asymptomatic (Table 2). However, *P. chlamydospora* and *P. minimum* DNA was detected in 100% of trunks (from 23 vines) sampled in the same field plot. Average quantity of *P. chlamydospora* and *P. minimum* DNA in the trunks was 3.6 ± 0.7 and 3.7 ± 0.9 (log (fg / ng of dry tissue))), respectively.

DISCUSSION

To date, no study has investigated leaf xylem water transport and vessel integrity during vascular pathogenesis using real time, non-invasive visualizations. Transplanting esca symptomatic vines (identified from years of survey) from the field to pots allowed the transport of the plants, enabling the use of synchrotron-based microCT to explore the relationship between vessel integrity and esca leaf symptom formation in intact vines at high resolution and in 3-dimensions. We demonstrate that gaseous embolism was not associated with esca leaf symptoms. Instead, most of the vessels in symptomatic leaves contained non-gaseous embolisms formed by gels and/or tyloses, hindering water transport and possibly leading to hydraulic failure. Nevertheless, there was no positive correlation between the severity of esca leaf symptoms and the loss of theoretical hydraulic conductivity resulting from these vascular occlusions. The two common vascular pathogens related to esca were undetected in the vine's distal organs (*i.e.* annual stems and leaves), confirming the symptoms and vascular occlusions occur at a distance from the pathogen niche localized in the trunk. Overall, these observations generate new perspectives regarding the nature and cause of esca leaf symptoms.

Native Embolism in Leaves

Vascular wilt diseases have been associated with significant levels of air embolism at the leaf level during oak bacterial leaf scorch (McElrone et al. 2008) and at the stem level during pine

wilt and Pierce's disease (Umebayashi et al. 2011; Kuroda 2012; Perez-Donoso et al. 2016). In these cases the formation of air embolism was speculated to result from the cell-wall degrading enzymatic activity of the pathogens (presumably to facilitate pathogen colonization through the vascular network). In our study there were extremely low levels of native gaseous embolism in both esca symptomatic and asymptomatic leaves (petioles and midribs), demonstrating symptom formation was not associated with the presence of air-filled vessels.

Leaf Xylem Occlusion: the Presence of Tyloses and Gels in Symptomatic Leaves

Under certain circumstances xylem vessels can be occluded by tyloses (outgrowths from adjacent parenchyma cells through vessel pits; Zimmermann 1979, De Micco et al. 2016), and/or gels (i.e. gums) composed of polysaccharides and pectins, which are secreted by parenchyma cells or directly by tyloses (Rioux et al. 1998). Tylose and/or gel formation is a general defense response of the plant against different biotic or abiotic stresses (Bonsen and Kučera 1990; Beckmann and Roberts 1995; Sun et al. 2008). In this study, microCT imaging of leaf xylem vessels (both in petioles and midribs) revealed all symptomatic leaves had occluded vessels, although the loss of theoretical hydraulic conductance resulting from these occlusions was highly variable between leaves. Using reconstructions of 3D microCT volumes (Figure 4) and light microscopy (Figure 5), we determined the occlusions in esca symptomatic leaves were due to both tyloses and gels. Numerous studies investigating vascular diseases have utilized artificial inoculation of the causal pathogen and observed the presence of vessel occlusions associated with decreases in hydraulic conductivity in either leaves or stems (Newbanks 1983; Choat et al. 2009; Collins et al. 2009; Pouzoulet et al. 2017). The artificial inoculation in these studies resulted in high levels of the pathogen at the same location as the observed vascular occlusions. During esca pathogenesis in naturally infected vines, xylem occlusions were observed in two-year old symptomatic branches and in roots, and the pathogens were detected at the same locations (Gómez et al. 2016). In the current study the two vascular pathogen species associated with esca trunk necroses, *P. chlamydospora* and *P. minimum*, were not detected in current year stems and leaves by a highly sensitive qPCR assay. This result was expected but had never been formally tested in the past according to the published literature. Thus, the vascular occlusions observed in leaves appeared to occur at some distance from the trunk where the necroses are usually observed and both of the fungal species were detected (Bruez et al. 2014, 2016; Morales-Cruz

et al. 2017; Massonnet et al. 2018), suggesting that vascular occlusions are caused by something else other than the fungi themselves.

Light microscopy and histochemical analyses showed occlusions are associated with the production of different compounds in symptomatic leaves: polysaccharides, including pectins and callose. Grapevine is known to accumulate polyphenolic compounds during *P. chlamydospora* and *Phaeoacremonium* spp. infections (Del Rio et al. 2001; Martin et al. 2009) and in esca symptomatic leaves (Valtaud et al. 2009; Valtaud et al. 2011; Martín et al. 2019). Also, it is well documented that gels are composed of pectins (Rioux et al. 1998), and that parenchyma cells and tyloses accumulate pectin during vessel occlusion (Clérivet et al. 2000). In their review, Beckmann and Roberts (1995) proposed a strong role of callose in tomato (*Solanum lycopersicum*) resistance to *Verticillium* spp., whereby callose xylem occlusions limit the spread of the pathogen. In the current study, the presence of tyloses and gels (of any chemical nature) not colocalized with pathogens suggests parenchyma cells play an important and active role during esca pathogenesis, expanding into the vessel lumen, secreting extracellular compounds, and eventually occluding the vessel.

Occlusions were clearly visible in partially-occluded vessels that embolized after cutting, and the contact angle between the outside wall of occlusions and the inner vessel wall ranged mostly from 120° to 150° (Figure 4E, 4F). This result suggests these occlusions are tyloses, as water droplets expanding into the vessels present lower contact angles (McCully et al. 2014).

Leaf Xylem Occlusion Occurs in Water-Filled Vessels

There are two main theories regarding the underlying mechanisms triggering vascular occlusion. Some studies have hypothesized the occlusions are always initiated by gaseous embolism and require the presence of air inside the vessel to stimulate the expansion of tyloses and/or the synthesis of gels (Zimmerman 1978; Canny 1997). Other studies suggest gaseous embolism is not required and instead occlusion formation is stimulated by the plant hormone ethylene (Perez-Donoso et al. 2006; Sun et al. 2007). Observations of samples fed with iohexol (Figure 4A) demonstrated occlusions were formed in water-filled vessels, suggesting gaseous embolism is not necessary to induce occlusion formation in esca symptomatic leaves. In grapevine, similar occlusions in water-filled vessels were identified

via microCT in grape berry pedicels associated with the onset of ripening (Knipfer et al. 2015).

The reconstruction of longitudinal sections of these vessels also demonstrated the flow pathway can be extremely reticulate, moving between adjacent vessels and around occluded portions. Complex flow pathways such as these have been suggested previously by microCT-based flow modeling in grape (Lee et al. 2013), but this is the first direct empirical evidence supporting these models. In grape berry pedicels partial occlusions are formed at the onset of ripening, yet despite a loss of conduit functionality, the pedicel hydraulic conductivity remained significantly high, suggesting a similar reticulate flow pathway in that context (Knipfer et al. 2015). The presence of partially-occluded vessels that still conduct water around occluded portions confirms occlusions were formed in functional water-filled vessels but creates difficulties with regards to interpreting images in cross section to determine vessel functionality. However, partially occluded vessels were found in very low percentage (1% in petioles and 8% in midribs, Supplemental Table S1) so they would not affect the loss of hydraulic conductivity estimated using microCT. In the current study we show examples of vessels that, when observed in a single cross section, appeared to be fully functional because of the clear iohexol signal (Figure 4 B,C). However, when more comprehensive analyses of the volume are made (e.g. here with >200 cross sections per microCT volume), it became apparent that the iohexol signal was sometimes found in between occlusions (Figure 4A). Therefore, quantifying occlusions from a limited number of cross sectional images could lead to an underestimation of the number of occluded vessels (as in Perez-Donoso et al. 2016). This is well-illustrated in our study where the percentage of occluded vessels in midribs of symptomatic leaves was underestimated (only 19.7%) when examining a limited number of light microscopy images compared to microCT image analyses. Even more problematic for magnetic resonance imaging (MRI) and microCT studies without the use of a mobile contrasting agent like iohexol, neither imaging technology appears capable of clearly distinguishing between functional, water-filled vessels and non-functional vessels filled by tyloses and/or gels. Only the use of robust volume analyses, in conjunction with contrasting agents, such as iohexol, can identify occlusions in apparently water-filled vessels. The presence of visible occlusions after cutting the sample (Figure 4E) complicates the interpretation regarding the effective functionality of the vessels. These partially-occluded vessels represented only a maximum of 8% of the total conductivity (Table S1) and should not significantly impact the overall PLC calculation. However, we can speculate embolisms

form even in these partially occluded vessels because: (i) the vessel was still partially functional with space between the visible occlusion and the vessel wall (e.g. in Figure 4E) yet the resolution of the scan was not sufficient enough to visualize this space, (ii) the water flow can "avoid" occlusions by passing through pits between vessels, or (iii) grapevine leaves are able to secrete gels and tyloses in a very short period, i.e. during the few minutes between the cut and the end of the scan. Since we never observed occlusions remaining in air-filled vessels in asymptomatic samples, this third possibility also implies symptomatic leaves are significantly more susceptible to occlusion than asymptomatic ones.

Leaf Symptoms, Occlusion, and Hypotheses on the Pathogenesis of Esca

Our results showed there was no significant correlation between the level of leaf necrosis and the level of occluded vessels in symptomatic leaf midribs and petioles. Similarly, it has been shown that during Pierce's disease in grapevine, leaf symptoms are not correlated with the presence of the bacterial pathogen (Gambetta et al. 2007). Although many symptomatic leaves exhibited high levels of occlusion, many did not, and even leaves with high levels of scorched area can exhibit low levels of occlusion. The absence of any relationship between these variables could suggest there is no causal relationship between xylem occlusions and esca leaf symptoms. However, it could have equally resulted because of the positions of our observations in relation to the way leaf necrosis proceeds. The current study may have missed even more significant levels of vascular occlusion localized just at the front of the leaf necrosis (secondary order veins). In addition, we demonstrated *P. chlamydospora* and *P. minimum* were not detected in the tissues of current year petioles and stems, but only in some of the 2-year old branches sampled and always in the trunks of symptomatic plants. All together these results demonstrate symptom development was associated with vascular occlusion that are likely elicited at a distance from the pathogen niche localised in the trunk.

Hypotheses on the pathogenesis of esca largely fall into two broad categories: 1) the hydraulic failure hypothesis where air embolism or vessel occlusion would disrupt the flow of sap in the xylem and lead to leaf desiccation, and 2) the elicitor-toxin hypothesis where elicitors/toxins produced by the pathogenic fungi or plant-derived signals move into the vine's transpiration stream inducing symptoms at a distance. The hydraulic failure hypothesis has never been properly tested, but observed decreases in stomatal conductance and photosynthesis in esca symptomatic leaves have been interpreted as supporting this

hypothesis (Petit et al. 2006; Andreini et al. 2009; Magnin-Robert et al. 2011). Some studies call this into question because water-stress related genes are not overexpressed during esca symptom formation (Letousey et al. 2010; Fontaine et al. 2016). The elicitor/toxin hypothesis is supported by numerous works that aimed to identify phytotoxins and effectors secreted by fungal pathogens associated with esca and their potential contributions in disease etiology (Abou-Mansour et al. 2004; Bruno et al. 2007; Bruno and Sparapano 2006; Luini et al. 2010; Masi et al. 2018). Other evidence is provided by the accumulation of antioxidant compounds prior to symptom expression in leaves (Valtaud et al. 2009; Magnin-Robert et al. 2011; Magnin-Robert et al. 2016). Esca pathogenesis could also involve plant-derived signals (e.g. hormones, defense molecules, etc.) triggering and/or accelerating leaf senescence (Haffner et al. 2015). Although esca leaf symptoms often take a form that differs from natural senescence, the role of the senescence program in esca pathogenesis should be more thoroughly studied in the future. Natural leaf senescence includes many of the same changes (e.g. Salleo et al. 2002; Brodribb and Holbrook 2003) that occur in esca symptomatic leaves: xylem vessel occlusion, decreases in stomatal conductance and photosynthesis, chlorosis, and eventually shedding. Authors have also suggested a role for the senescence program in Pierce's disease pathogenesis (Choat et al. 2009).

The results presented here are consistent with the hypothesis that esca pathogens are restricted to the trunk and/or multi-year branches and that elicitors and/or toxins (reviewed in Andolfi et al. 2011) become systematic in the plant via the transpiration stream, accumulate in the canopy, and trigger a cascade of events that lead to visual symptoms. These events include the production of tyloses and gels by the plant that occlude vessels, suggesting the elicitor/toxin and hydraulic failure hypotheses are not necessarily mutually exclusive. This is also congruent with the observation of necrosis/oxidation along the vasculature that is spatially associated with leaf symptoms (Lecomte et al. 2012). The precise timing and direct impact of vessel occlusion relative to symptom formation remains unclear so the current study cannot determine whether occlusions lead to hydraulic failure and symptom formation, or whether the observed vessel occlusion is simply a result of an early induced senescence process. Future research should be aimed at exploring this sequence of events leading to leaf scorch symptoms in naturally infected esca symptomatic vines in the field.

MATERIALS and METHODS

Plant Material

Grapevine (*Vitis vinifera* cv. Sauvignon blanc) plants aged 27 years old were transplanted from the field into pots from a vineyard at INRA Aquitaine (44°47'24.8"N, 0°34'35.1"W). The transplantation was the only method allowing the study of natural esca symptom development on mature plants outside the field (greenhouse and synchrotron) and to bring the plants from Bordeaux (INRA) to Paris (synchrotron SOLEIL). The experimental plot included 343 plants organized in 8 rows surveyed each season before transplantation for esca leaf symptom expression during the previous 5 to 6 years following Lecomte et al. (2012) leaf scorch symptom description. Esca incidence in this vineyard was very high as 77% of the plants (n=343 plants) presented trunks and/or leaf symptoms the summer before the plants were uprooted. The presence of two vascular fungi associated with esca (*Phaeomoniella chlamydospora* and *Phaeoacremonium minimum*) in this plot was confirmed by using qPCR on the trunk of 23 symptomatic vines randomly sampled (methodology described below). To reduce stressful events the plants were excavated during dormancy before bud burst in late winter from the field by digging around the woody root system and attempting to preserve as many of the large woody roots as possible. Following excavation the root system was immersed under water overnight, and then powdered with acid indol-3-butyric to promote rooting. To equilibrate the vigor of the plants and their leaf/root ratio, three to five buds per arm (one per side) were left. The plants were potted in 20-l pots in fine clay medium (Klasmann Deilmann substrat 4: 264) and placed indoors for two months on heating plates (30°) to encourage root development before they were transferred to a greenhouse and irrigated to capacity every other day under natural light. Plants were irrigated with nutritive solution [0.1 mM $NH_4H_2PO_4$, 0.187 mM NH_4NO_3, 0.255 mM KNO_3, 0.025 mM $MgSO_4$, 0.002 mM Fe, and oligo-elements (B, Zn, Mn, Cu, and Mo)] to prevent mineral deficiencies. Plants were grown in a greenhouse and exposed to natural light. Temperature and air relative humidity were monitored every 30 min: average daily values corresponded to 26 ± 4 (SE) °C, and 64 ± 13% (SE), respectively. Leaf predawn water potential (Ψ_{PD}) was monitored regularly to ensure the plants were never water-stressed (Ψ_{PD} close to 0 MPa). The plants were surveyed weekly for esca leaf symptom development from May to September. The plants were noted as symptomatic when at least 50% of the canopy was presenting the tiger-stripe leaf symptom, characteristic for esca (see examples of leaf symptoms in Supplemental Figure S5A and entire plants in Supplemental Figure S5B). Six plants were selected (Table 3) and transferred to the microCT PSICHE beamline (SOLEIL synchrotron facility, Saclay,

France): two control asymptomatic plants that had never expressed symptoms either during the year of the experiment or the past five years, and four symptomatic plants with differences in the timing of the first leaf symptom expression (6, 5, 4, and 2 weeks before the experiment). Leaf symptoms (Supplemental Figure S5) were typical esca leaf symptoms for Sauvignon blanc and were similar to the symptoms we observed in the experimental vineyard from which the plants came. All symptomatic plants had expressed esca symptoms for at least three different seasons in the past (Table 3). Asymptomatic leaves were always sampled only from the control plants A1 and A2.

MicroCT

Synchrotron-based X-ray micro-computed tomography (microCT) was used to visualize the contents of vessels in the esca symptomatic and asymptomatic leaf midribs and petioles. The PSICHE beamline (Pressure Structure Imaging by Contrast at High Energy) at SOLEIL synchrotron facility (Saclay, France) that is dedicated to x-ray diffraction under extreme conditions (pressure-temperature) and to high energy absorption contrast tomography (20-50 keV) was used (King et al. 2016). During the first campaign in September 2017, one 26-year-old plant presenting characteristic tiger-stripe leaf symptoms was scanned with the microCT PSICHE beamline (King et al. 2016). In the second campaign, in September 2018, 5 different plants of the same age (2 asymptomatic and 3 symptomatic) were brought to the same facility. Intact shoots (>1.5m in length) were cut at the base under water and leaves, at least 1m away from the scanned leaves and scanned using a high-flux (3×10^{11} photons mm^{-2}) 25-keV monochromatic X-ray beam. Midribs (n=21) and petioles (n=15) were scanned in symptomatic and asymptomatic leaves (from 1 to 5 leaves per plant), then cut just above the scanned area and scanned again. The projections were recorded with a Hamamatsu Orca Flash sCMOS camera equipped with a 250-µm-thick LuAG scintillator for petioles and with a 90-µm-thick LuAG scintillator for midribs. The complete tomographic scan included 1500 projections, and each projection lasted 50 ms for petioles and 200 ms for midribs. Thus, the total exposure time was 75 s for petioles and 300 s for midribs. Tomographic reconstructions were performed using PyHST2 software (Mirone et al., 2014) using the Paganin method (Paganin et al., 2002), resulting in 32-bit volume reconstructions of 2048 x 2048 x 1024 voxels for petioles and 2048 x 2048 x 2048 voxels for midribs. The final spatial resolution was 2.8769^3 μm^3 per voxel for petioles and 0.8601^3 μm^3 for midribs.

Iohexol Contrasting Agent

A subset of ten shoots were fed with the contrasting agent iohexol. Five symptomatic (from two plants: S1 and S2 described in Table 3) and five asymptomatic shoots (from two plants: A1 and A2 described in Table 3) were cut at the base under water and immediately transferred to a solution containing the contrasting agent iohexol [150mM] to visualize functional (*i.e.* vessels that were effectively transporting sap; Pratt and Jacobsen 2018). In asymptomatic plants 5 midribs (from 3 different shoots) and 3 petioles (from 2 different shoots) and in symptomatic plants, 5 midribs (from 3 different shoots) and 4 petioles (from 3 different shoots) were scanned. These shoots were exposed to sunlight outdoors for at least half a day to permit the contrast agent to reach the leaves through transpiration. The capacity and rapidity of iohexol to move was first checked by cutting leaves under water, submerging them directly in iohexol solution and scanning several times each 10 min. Its capacity to move up to the shoots was then checked by scanning leaves at the top. These results were not coupled with the ones from intact leaf scans. In this case scans were performed at two different energies, just below and just above the iodine K-edge of 33.2 keV. At 33.1 keV the contrast agent presents little contrast while it presents strong contrast at 33.3 keV. The leaves (17 of 35 total samples) were then analyzed in the beamline as described for the other samples above.

Image Analysis

Leaf Symptoms

Scanned leaves were photographed, and the green area was calculated using G. Landini plug-in threshold_color v1.15 (http://www.mecourse.com/landinig/software/software.html) in ImageJ software (http://rsb.info.nih.gov/ij), differentiating four color regions: red, yellow, pale green, and green. The number of pixels for each region was summed to determine the leaf area corresponding to each color region. To obtain a scale of symptom severity, the percentage of green leaf area (relative to total leaf area) was calculated for each leaf.

Analysis of microCT Images

All samples (including those stained with iohexol) were analyzed in the following manner. The geometrical diameter of air- and non-air-filled vessels were measured on cross sections taken from the central slice of the microCT scanned volume using ImageJ software. For iohexol-fed samples an example of vessel identification is included in Supplemental Figure S6. The theoretical hydraulic conductivity of each vessel was calculated using the Hagen-Poiseuille equation.

$$[1]\ Kh = (\pi * ø^4 * \rho) / (128 * \eta)$$

Where Kh is the theoretical hydraulic conductivity (m^4 MPa^{-1} s^{-1}), $ø$ is the geometrical diameter of the vessel (m), ρ is the density of water (Kg m^{-3}), and η the viscosity of water (1.002 mPa s^{-1} at 20 °C). The percentage of native embolism was calculated in the first scan, before cutting the leaf, using the following equation:

$$[2]\ Native\ PLC\ (\%) = 100 * (\Sigma\ Kh_{air\ filled\ vessels}) / (\Sigma\ Kh_{all\ vessels})$$

After a first scan the samples were cut with a clean razor blade just above the scanned area and scanned again. Cut open vessels will embolize because the xylem sap is under negative pressure. Leaf water potential (Ψ_L) measured on an adjacent leaf just after the scan indicated sufficient tension in the xylem sap to embolize in all leaves measured (n=17 leaves, Ψ_L=-0.46 MPa on average). Under control conditions nearly all the xylem vessels became air-filled upon cutting (*e.g.* black vessels in Figure 1B, Supplemental Figure S1B). To estimate the loss of conductivity caused by occluded vessels (equation 3 below), the Kh of apparent water-filled vessels was calculated in the central cross section of the entire microCT volume after cutting. Vessels that did not become completely air-filled after cutting were considered occluded (*i.e.* having the same grey level after cutting as water-filled conduit before cutting). To adjust PLC (equation[*3*] presented below) by those vessels that appeared water-filled or air-filled only at specific points along the length of the vessel, the presence of apparent water-filled vessels and droplets was checked in at least 200 cross sectional slices in each volume; corresponding to 160 µm for midribs and 570 µm for petioles. If a particular vessel appeared water-filled in any of the 200 slices examined, this vessel was classified as partially-occluded and added to the PLC given by occlusions.

$$[3]\ Occlusion\ PLC\ (\%) = 100 * (\Sigma Kh_{occluded\ vessels} + \Sigma\ Kh_{partially\ occluded\ vessels}) / (\Sigma\ Kh_{all\ vessels})$$

Contact Angles

To gain insight into the nature of occlusion, the contact angle between each droplet and the inner vessel wall was measured using ImageJ following McCully et al. (2014). First longitudinal slices were reconstructed from each microCT volume. Then the contact angles between each observed droplet and the vessel wall were measured in partially-occluded, air-filled vessels (n = 190 droplets from 65 partially-occluded vessels in 2 different samples).

Light Microscopy

Ten millimeter sections from midribs and petioles of 3 esca symptomatic and 3 asymptomatic leaves were cut and fixed in a solution containing 0.64% (v/v) paraformaldehyde, 50% (v/v) ethanol, 5% (v/v) acetic acid, and 44.36% (v/v) water. Samples were then dehydrated using a graded series of ethanol (50%, 70%, 85%, 95%, 100%, 100%, and 100% (v/v) for 30 min each) and embedded using a graded series of LR White resin (Agar scientific, Stansted, UK) (33%, 50%, 66% (v/v) L.R. White in ethanol solutions for 120 min. each, and 100% (v/v) LR White three times overnight). Two to 2.5 µm thick transverse sections were cut using an Ultracut S microtome (Reichert, Vienna, Austria) equipped with a glass knife. As described in Neghliz et al. (2016), the cross section was stained with different dyes. To investigate anatomical features, lignin, phenolic compounds, and polysaccharides cross sections were stained with 0.05% (w/v) toluidine blue O. Sections to be examined for polysaccharides were stained with periodic acid-Schiff's reagent. Pectins were detected by staining sections overnight with 1% (w/v) ruthenium red. Callose was revealed by staining sections overnight with 1% (w/v) lacmoid blue in 3% (v/v) acetic acid. Stained sections were dried and photographed with a RTKE camera (Spot, Sterling Heights, MI, USA) mounted on an Axiophot microscope (Zeiss, Jena, Germany) at the Bordeaux Imaging Center, member of the France Bio Imaging national infrastructure (ANR-10-INBS-04). In midribs, the image of the entire cross section was analyzed to quantify the percentage of occluded vessels (by tyloses, gels, or both) in 55 sections for symptomatic and 56 for asymptomatic midribs obtained from 6 different leaves (3 symptomatic and 3 asymptomatic). Occlusions were classified as tyloses if tylose cell walls (formed during tylosis development) were visualized within the vessel lumen (*e.g.* Fig. 5B) or gels if cell walls were not visualized and the vessel lumen appeared

totally filled (*e.g.* Fig 5A red arrows). Tyloses and gels can also be observed within the same vessel (*e.g.* Fig. 5D). In some cases tyloses and gels can be difficult to distinguish if tyloses filled the entire vessel lumen with a wall closely attached to the inner vessel wall, or if the tyloses wall is lignified. However this uncertainty would not change the total number of occluded vessels observed in the present study.

Fungal Detection

Presence of *P. chlamydospora* and *P. minimum* was assessed in different parts of asymptomatic and symptomatic plants. Plants were sampled directly from the same field plot as described above. In mid-august of 2018, a survey of leaf esca symptoms was conducted and 6 asymptomatic and 6 symptomatic vines were selected at random. Four different samples were collected for each plant: (i) petioles of three leaves located in the first 50 cm of the shoot, sections of the (ii) first and (iii) fifth internodes of the third shoot on the two year-old cane, and (iv) a section of the two-year old branch just basal to the third shoot (i.e. canes trained across in the "Guyot" system). These organs were focused on as they are typically not used to detect esca pathogens, which have mainly been observed in the trunk. However, to control the presence of these fungi in the trunk, 23 symptomatic plants were randomly sampled from the same plot by drilling 1cm at the same height in each trunk. All samples were collected using ethyl-alcohol sterilized pruning shears and placed immediately in liquid nitrogen. DNA extraction and qPCR analysis were conducted as previously described by Pouzoulet et al. 2013, 2017, using the primer sets PchQF/R and PalQF/R. Briefly, samples were lyophilized for 48h. After the bark and pith were removed from the samples (except for petioles) using a sterile scalpel, samples were ground, and DNA was extracted as described by Pouzoulet et al. 2013. Quantification of *P. chlamydospora* and *P. minimum* DNA by qPCR (SYBR-Green assays) was conducted as described by Pouzoulet et al. 2017. Pathogen DNA quantity was normalized by the amount of total DNA used as template, and the mean of three technical replicates was used for further analysis.

Statistical Analysis

The effects of leaf symptom (A: asymptomatic, S: symptomatic), organ (midrib or petiole), and their interaction on the calculated native percentage loss of hydraulic conductivity (*i.e.* native PLC, %) and on the percentage loss of theoretical hydraulic conductivity due to

occluded vessels (*i.e*. occlusion PLC, %) was tested using PROC GLIMMIX in SAS software (SAS 9.4; SAS Institute, Cary, NC, USA). The plant was entered into models as a random effect since different leaves were sometimes scanned from the same plant (from 1 to 5 per plant). Proportional data (ranging from 0 to 1, dividing all PLC data by 100) was analyzed to fit a logit link function and binomial distribution as appropriate. We computed pairwise least squares means differences of fixed effects. The effect of symptom severity (expressed as the percentage of green tissue) among symptomatic leaves on PLC was tested as described above including the plant and organ as covariables (fixed effects) in the model.

SUPPLEMENTAL DATA

Supplemental Figure S1. Two-dimensional reconstructions of cross sections from microCT volumes and optical microscopy cross sections of *V. vinifera* leaf petioles.

Supplemental Figure S2. Two-dimensional reconstructions of longitudinal and cross sections from microCT volumes of *V. vinifera* leaf midribs.

Supplemental Figure S3. Two-dimensional reconstructions of longitudinal and cross sections from microCT volumes for esca asymptomatic leaf midribs scanned on iohexol-fed *V. vinifera* shoots.

Supplemental Figure S4. Light microscopy images of cross sections of esca asymptomatic midribs of *V. vinifera*.

Supplemental Figure S5. Pictures of asymptomatic control and esca symptomatic plants of *V. vinifera* cv. Sauvignon blanc.

Supplemental Figure S6. Method used for vessel segmentation in iohexol-fed *V. vinifera* petioles.

Supplemental Table S1 Calculated theoretical conductivity (% Kh) from microCT volumes.

Supplemental Table S2 Quantification of not-filled and occluded vessels in histological photomicrograph of *V. vinifera* midribs.

ACKNOWLEDGEMENTS

We thank the experimental teams of UMR SAVE and UMR EGFV (Bord'O platform, INRA, Bordeaux, France) and the SOLEIL synchrotron facility (HRCT beamline PSICHE) for providing the materials and logistics. We thank J. Jolivet for providing technical knowledge and support for plant transplantation and B. Batailler from the Bordeaux Imaging Center for

providing technical support for the light microscopy sample preparation. This study was conducted with financial support from the French Ministry of Agriculture (FranceAgriMer and CNIV) within the PHYSIOPATH project (program "Plan National issement du Vignoble"), the Cluster of Excellence COTE (ANR-10-LABX-45, within the VIVALDI and DEFI projects), the programme 'Investments for the Future' (ANR-10-EQPX-16, XYLOFOREST), and the AgreenSkills Fellowship program, which has received funding from the European Union's Seventh Framework Program under grant agreement no. FP7 26719 (AgreenSkills contract 688 for G.C.).

TABLES

Table 1. Effects of esca leaf symptom (asymptomatic or symptomatic), organ (midrib or petiole), and their interaction on the calculated native percentage loss of hydraulic conductivity due to native embolism (Native PLC, %) and on the calculated percentage loss of hydraulic conductivity due to occlusions (Occlusion PLC, %). The plant was entered as a random effect in the models. Statistically significant results (*P*-value < 0.05) are shown in bold. See the text for the model specificity for each trait.

Response variable	Explanatory variables	*F*-value	*P*-value
Native PLC (%) n=35	Leaf symptom	1.06	0.36
	Organ	0.37	0.61
	Interaction	2.53	0.25
Occlusion PLC (%) n=35	Leaf symptom	**14.32**	**0.02**
	Organ	1.99	0.29
	Interaction	0.61	0.52

Table 2. Quantification by qPCR of *Phaeomoniella chlamydospore (P.ch)* and *Phaeoacremonium minimum (P.min)* (log (fg of pathogen DNA / ng of dry tissue)). High quantity of the DNA of the two pathogens was confirmed in 100% of the trunks of symptomatic plants sampled from the same vineyard (n=23, see text for details). Values represent means ± standard error in different organs, n=sample size, Esca leaf symptom: S=symptomatic A=asymptomatic.

Pathogen	n	Esca	Petiole	1st internode	5th internode	Multi-year branches
P.ch	6	S	0	0	0	1.05 ± 0.58 (3/6)*
P.ch	6	A	0	0	0	1.13 ± 0.38 (4/6)*
P.min	6	S	0	0	0	1.48 ± 0.75 (3/6)*
P.min	6	A	0	0	0	0.59 ± 0.37 (2/6)*

*Number of samples positive for the pathogen

Table 3 Disease history of the *V. vinifera* cv. Sauvignon blanc plants used in this study. Symptom frequency over time indicates the number of years with symptoms over the 6 or 5 years before transplantation.

Plant	Year of transplantation	Symptom frequency over time (number of years)	Duration of leaf symptoms (weeks) prior to the moment of the experiment
A1	2018	0/6	0
A2	2018	0/6	0
S1	2018	4/6	2
S2	2018	6/6	4
S3	2018	5/6	6
S4	2017	5/5	5

FIGURE LEGENDS

Figure 1. Two-dimensional reconstructions of cross sections from microCT volumes of *V. vinifera* leaves. Esca asymptomatic (**A**, **B**) and esca symptomatic (**C**, **D**) leaf midribs of *V. vinifera* plants. After a first scan on intact leaves (**A, C**) the samples were cut (**B, D**) just above the scanned area to embolize the vessels and then scanned again. Air-filled (*e.g.* black arrows), water-filled (*e.g.* white arrows), and occluded (*e.g.* red arrows) vessels were counted and their cross-sectional diameters quantified to determine the percentage loss of conductivity (PLC). The PLC represented by either native embolism (**A**, **C**) or occluded vessels (**B**, **D**) is given in parentheses. Scale bar = 100µm.

Figure 2. Mean native PLC in midribs and petioles of esca asymptomatic (blue) and esca symptomatic (red) leaves of *V. vinifera* plants using microCT imaging. PLC was calculated from the diameter of air-filled vessels in intact leaves, based on the total theoretical hydraulic conductivity of each sample. Error bars represent ± standard errors and different letters represent statistically significant differences (least squares means differences of fixed effects, P-value < 0.05, n=sample size).

Figure 3. Mean occlusion PLC in midribs and petioles of esca asymptomatic (blue) and esca symptomatic (red) leaves of *V. vinifera* plants using microCT imaging. PLC was calculated from the diameter of occluded vessels, based on the total theoretical hydraulic conductivity of each sample. Error bars represent ± standard errors and different letters represent statistically significant differences (least squares means differences of fixed effects, P-value < 0.05, n=sample size).

Figure 4. Two-dimensional reconstructions from microCT volumes of esca symptomatic leaves of *V. vinifera*. (**A-C**) Iohexol-fed midrib viewed in a longitudinal (**A**) and cross sections (**B**, **C**). For clarity and orientation the same three vessels are color coded and dotted lines represent the location of the sections relative to each other. The contrasting agent iohexol appears bright white and allows for the identification of the water transport pathway. The iohexol signal can even be seen in partially-occluded vessels (e.g. white arrow). Occlusions (i.e. gels or tyloses) can span the entire diameter of the vessel (red arrows) or only a portion (yellow arrows). After a first scan on intact leaves (**A, B**), the sample was cut (**C**) just above the scanned area and scanned again. (**D**) Longitudinal-section of a midrib with

completely occluded vessels; the presence of occlusions are visible (although obscure) inside the vessel lumen (red arrows). (**E**) Longitudinal-section of an air-filled midrib (after cutting) with clearly visible occlusions (red arrows). (**F**) Frequency distribution of the contact angles between the occlusions and the vessel wall (sample size=190). Scale bars=100µm.

Figure 5. Light microscopy images of cross sections of esca symptomatic midribs of *V. vinifera*. Cross-sections were stained with toluidine blue O (**A**), periodic-acid Schiff's reactive (**B**), ruthenium red (**C**), and lacmoid blue (**D**). Red arrows indicate the presence of gels filling entirely the vessel lumen while black arrows indicate the presence of tyloses in vessel lumina. Scale bars = 100µm.

Figure 6. Relationship between the esca symptom severity (expressed as % green tissue per leaf) and the theoretical loss of hydraulic conductivity due to occluded vessels (occlusion PLC) in midribs and petioles of *V. vinifera*. Points are grouped by plant: A1, A2 (blue, asymptomatic), S1-S4 (red, symptomatic). The relationship between PLC and green tissue is not significant among symptomatic samples (red points, *P*-value=0.25).

LITERATURE CITED

Abou-Mansour, E., Couché, E., Tabacchi, R., 2004. Do fungal naphthalenones have a role in the development of esca symptoms? Phytopathologia Mediterranea 43, 75–82. http://dx.doi.org/10.14601/Phytopathol_Mediterr-1728

Andolfi, A., Mugnai, L., Luque, J., Surico, G., Cimmino, A., Evidente, A., 2011. Phytotoxins produced by fungi associated with grapevine trunk diseases. Toxins 3, 1569–1605. https://doi.org/10.3390/toxins3121569

Andreini, L., Caruso, G., Bertolla, C., Scalabrelli, G., Viti, R., Gucci, R., 2009. Gas exchange, stem water potential and xylem flux on some grapevine cultivars affected by esca disease. South African Journal of Enology & Viticulture 30. https://doi.org/10.21548/30-2-1434

Beckman, C.H., Roberts, E.M., 1995. On the nature and genetic basis for resistance and tolerance to fungal wilt diseases of plants, in: Advances in Botanical Research. Elsevier, pp. 35–77. https://doi.org/10.1016/S0065-2296(08)60008-7

Bertsch, C., Ramírez-Suero, M., Magnin-Robert, M., Larignon, P., Chong, J., Abou-Mansour, E., Spagnolo, A., Clément, C., Fontaine, F., 2013. Grapevine trunk diseases: complex and still poorly understood. Plant Pathology 62, 243–265. https://doi.org/10.1111/j.1365-3059.2012.02674.x

Bonsen, K.J.M., Kučera, L.J., 1990. Vessel Occlusions in Plants: Morphological, Functional and Evolutionary Aspects. IAWA Journal 11, 393–399. https://doi.org/10.1163/22941932-90000528

Brodribb, T.J., Holbrook, N.M., 2003. stomatal closure during leaf dehydration, correlation with other leaf physiological traits. Plant Physiology 132, 2166–2173. https://doi.org/10.1104/pp.103.023879

Bruez, E., Baumgartner, K., Bastien, S., Travadon, R., Guérin-Dubrana, L., Rey, P. 2016. Various fungal communities colonise the functional wood tissues of old grapevines externally free from grapevine trunk disease symptoms. Australian journal of grape and wine research, 22: 288-295. https://doi.org/10.1111/ajgw.12209

Bruez, E., Vallance, J., Gerbore, J., Lecomte, P., Da Costa, J.-P., Guerin-Dubrana, L., Rey, P., 2014. Analyses of the temporal dynamics of fungal communities colonizing the healthy wood tissues of esca leaf-symptomatic and asymptomatic vines. PLoS ONE 9, e95928. https://doi.org/10.1371/journal.pone.0095928

Bruno, G., Sparapano, L., 2006. Effects of three esca-associated fungi on *Vitis vinifera* L.: III. Enzymes produced by the pathogens and their role in fungus-to-plant or in fungus-to-fungus interactions. Physiological and Molecular Plant Pathology 69, 182–194. https://doi.org/10.1016/j.pmpp.2007.04.006

Bruno, G., Sparapano, L., Graniti, A., 2007. Effects of three esca-associated fungi on *Vitis vinifera* L.: IV. diffusion through the xylem of metabolites produced by two tracheiphilous fungi in the woody tissue of grapevine leads to esca-like symptoms on leaves and berries. Physiological and Molecular Plant Pathology 71, 106–124. https://doi.org/10.1016/j.pmpp.2007.12.004

Canny, M., 1997. Tyloses and the maintenance of transpiration. Annals of Botany 80, 565–570. https://doi.org/10.1006/anbo.1997.0475

Choat, B., Gambetta, G.A., Wada, H., Shackel, K.A., Matthews, M.A., 2009. The effects of Pierce's disease on leaf and petiole hydraulic conductance in *Vitis vinifera* cv. Chardonnay. Physiologia Plantarum 136, 384–394. https://doi.org/10.1111/j.1399-3054.2009.01231.x

Clérivet, A., Déon, V., Alami, I., Lopez, F., Geiger, J.-P., Nicole, M., 2000. Tyloses and ggels associated with cellulose accumulation in vessels are responses of plane tree seedlings (Platanus × acerifolia) to the vascular fungus *Ceratocystis fimbriata* f. sp platani. Trees 15, 25–31. https://doi.org/10.1007/s004680000063

Cloete, M., Mostert, L., Fischer, M., Halleen, F. 2015. Pathogenicity of South African Hymenochaetales taxa isolated from esca-infected grapevines. Phytopathologia Mediterranea 54, 368-379. https://doi.org/10.14601/Phytopathol_Mediterr-16237

Collins, B.R., Parke, J.L., Lachenbruch, B., Hansen, E.M., 2009. The effects of *Phytophthora ramorum* infection on hydraulic conductivity and tylosis formation in tanoak sapwood. Canadian Journal of Forest Research 39, 1766–1776. https://doi.org/10.1139/X09-097

Del Rio, J.A., Gonzalez, A., Fuster, M.D., Botia, J.M., Gomez, P., Frias, V., Ortuno, A., 2001. Tylose formation and changes in phenolic compounds of grape roots infected with *Phaeomoniella chlamydospora* and *Phaeoacremonium* species. Phytopathologia Mediterranea 40, S394–S399. http://dx.doi.org/10.14601/Phytopathol_Mediterr-1644

De Micco, V., Balzano, A., Wheeler, E. A., & Baas, P. 2016. Tyloses and gums: a review of structure, function and occurrence of vessel occlusions. IAWA journal 37, 186-205. http://dx.doi.org/10.1163/22941932-20160130

Feliciano, A. J., Eskalen, A., Gubler, W. D., 2004. Differential susceptibility of three grapevine cultivars to the *Phaeoacremoium aleophilum* and *Phaeomoniella chlamydospora* in California. Phytopathologia Mediterranea 43, 66-69. http://dx.doi.org/10.14601/Phytopathol_Mediterr-1727

Fischer, M., 2006. Biodiversity and geographic distribution of basidiomycetes causing esca-associated white rot in grapevine: a worldwide perspective. Phytopathologia Mediterranea 45, S30-S42.http://dx.doi.org/10.14601/Phytopathol_Mediterr-1846

Fischer, M., Peighami-Ashnaei, S. 2019. Grapevine, esca complex, and environment: the disease triangle. Phytopathologia Mediterranea 58, 17-37. http://dx.doi.org/10.14601/Phytopathol_Mediterr-25086

Fisher, P.J., Petrini, O., Sutton, B.C., 1993. A comparative study of fungal endophytes in leaves, xylem and bark of Eucalyptus in Australia and England. Sydowia 45, 338–345.

Fontaine, F., Pinto, C., Vallet, J., Clément, C., Gomes, A.C., Spagnolo, A., 2016. The effects of grapevine trunk diseases (GTDs) on vine physiology. European Journal of Plant Pathology 144, 707–721. https://doi.org/10.1007/s10658-015-0770-0

Fradin, E. F., Thomma, B. P., 2006. Physiology and molecular aspects of *Verticillium* wilt diseases caused by *V. dahliae* and *V. albo-atrum*. Molecular plant pathology 7, 71-86. https://doi.org/10.1111/j.1364-3703.2006.00323.x

Gambetta, G.A., Fei, J., Rost, T.L., Matthews, M.A., 2007. Leaf scorch symptoms are not correlated with bacterial populations during Pierce's disease. Journal of Experimental Botany 58, 4037–4046. https://doi.org/10.1093/jxb/erm260

Gómez, P., Báidez, A.G., Ortuño, A., Del Río, J.A., 2016. Grapevine xylem response to fungi involved in trunk diseases: Grapevine vascular defence. Annals of Applied Biology 169, 116–124. https://doi.org/10.1111/aab.12285

Guerin-Dubrana, L., Fontaine, F., Mugnai, L. 2019. Grapevine trunk disease in European and Mediterranean vineyards: occurrence, distribution and associated disease-affecting cultural factors. Phytopathologia Mediterranea 58, 49-71. https://doi.org/10.13128/Phytopathol_Mediterr-25153

Gramaje, D., Úrbez-Torres, J.R., Sosnowski, M.R., 2018. Managing grapevine trunk diseases with respect to etiology and epidemiology: current strategies and future prospects. Plant Disease 102, 12–39. https://doi.org/10.1094/PDIS-04-17-0512-FE

Hochberg, U., Windt, C.W., Ponomarenko, A., Zhang, Y-J., Gersony, J., et al. 2017. Stomatal closure, basal leaf embolism and shedding protect the hydraulic integrity of grape stems. Plant Physiologist, 174: 764–75. https://doi.org/10.1104/pp.16.01816

Häffner, E., Konietzki, S., Diederichsen, E., 2015. Keeping control: the role of senescence and development in plant pathogenesis and defense. Plants 4, 449–488. https://doi.org/10.3390/plants4030449

King, A., Guignot, N., Zerbino, P., Boulard, E., Desjardins, K., Bordessoule, M., Leclerq, N., Le, S., Renaud, G., Cerato, M., Bornert, M., Lenoir, N., Delzon, S., Perrillat, J.-P., Legodec, Y., Itié, J.-P., 2016. Tomography and imaging at the PSICHE beam line of the SOLEIL synchrotron. Review of Scientific Instruments 87, 093704. https://doi.org/10.1063/1.4961365

Knipfer, T., Fei, J., Gambetta, G. A., McElrone, A. J., Shackel, K. A., Matthews, M. A. 2015. Water transport properties of the grape pedicel during fruit development: insights into xylem anatomy and function using microtomography. Plant Physiology 168, 1590-1602. https://doi.org/10.1104/pp.15.00031

Kuroda, K., 2012. Monitoring of xylem embolism and dysfunction by the acoustic emission technique in *Pinus thunbergii* inoculated with the pine wood nematode *Bursaphelenchus xylophilus*. Journal of Forest Research 17, 58–64. https://doi.org/10.1007/s10310-010-0246-1

Larignon, P. and Dubos, B., 1997. Fungi associated with esca disease in grapevine. European Journal of Plant Pathology 10, 147-157. https://doi.org/10.1023/A:1008638409410

Lecomte, P., Darrieutort, G., Liminana, J. M., Comont, G., Muruamendiaraz, A., Legorburu, F. J., Choueiri, E., Jreijiri, F., El Amil, R., Fermaud, M., 2012. New insights into esca of grapevine: the development of foliar symptoms and their association with xylem discoloration. Plant Disease 96, 924-934. https://doi.org/10.1094/PDIS-09-11-0776-RE

Lee, E.F., Matthews, M.A., McElrone, A.J., Phillips, R.J., Shackel, K.A., Brodersen, C.R., 2013. Analysis of HRCT-derived xylem network reveals reverse flow in some vessels. Journal of Theoretical Biology 333, 146–155. https://doi.org/10.1016/j.jtbi.2013.05.021

Letousey, P., Baillieul, F., Perrot, G., Rabenoelina, F., Boulay, M., Vaillant-Gaveau, N., Clément, C., Fontaine, F., 2010. Early events prior to visual symptoms in the apoplectic form of grapevine esca disease. Phytopathology 100, 424-431. https://doi.org/10.1094/PHYTO-100-5-0424

Luini, E., Fleurat-Lessard, P., Rousseau, L., Roblin, G., Berjeaud, J.-M., 2010. Inhibitory effects of polypeptides secreted by the grapevine pathogens Phaeomoniella chlamydospora and Phaeoacremonium aleophilum on plant cell activities. Physiological and Molecular Plant Pathology 74, 403–411. https://doi.org/10.1016/j.pmpp.2010.06.007

Magnin-Robert, M., Letousey, P., Spagnolo, A., Rabenoelina, F., Jacquens, L., Mercier, L., Clément, C., Fontaine, F., 2011. Leaf stripe form of esca induces alteration of photosynthesis and defence reactions in presymptomatic leaves. Functional Plant Biology 38. https://doi.org/10.1071/FP11083

Magnin-Robert, M., Spagnolo, A., Boulanger, A., Joyeux, C., Clément, C., Abou-Mansour, E., Fontaine, F., 2016. Changes in plant metabolism and accumulation of fungal metabolites in response to esca proper and apoplexy expression in the whole grapevine. Phytopathology 106, 541–553. https://doi.org/10.1094/PHYTO-09-15-0207-R

Martín, L., Fontaine, F., Castaño, F.J., Songy, A., Roda, R., Vallet, J., Ferrer-Gallego, R., 2019. Specific profile of Tempranillo grapevines related to Esca-leaf symptoms and climate conditions. Plant Physiology and Biochemistry 135, 575–587. https://doi.org/10.1016/j.plaphy.2018.10.040

Martin, N., Vesentini, D., Rego, C., Monteiro, S., Oliveira, H., Ferreira, R.B., 2009. *Phaeomoniella chlamydospora* infection induces changes in phenolic compounds content in *Vitis vinifera*. Phytopathologia Mediterranea 48, 101–116. http://dx.doi.org/10.14601/Phytopathol_Mediterr-2879

Masi, M., Cimmino, A., Reveglia, P., Mugnai, L., Surico, G. and Evidente, A. 2018. Advances on fungal phytotoxins and their role in grapevine trunk diseases. Journal of agricultural and food chemistry 66, 5948-5958. https://doi.org/10.1021/acs.jafc.8b00773

Massonnet., M., Morales-Cruz, A., Minio A., Figueroa-Balderas, R., Lawrence, D.P., Travadon, R., Rolshausen, P.E., Baumgartner, K., Cantu, D., 2018. Whole-genome resequencing and pan-transcriptome reconstruction highlight the impact of genomic structural variation on secondary metabolite gene clusters in the grapevine esca pathogen *Phaeoacremonium minimum*. Frontiers in Microbiology 9, 1784. https://doi.org/10.3389/fmicb.2018.01784

McCully, M., Canny, M., Baker, A., Miller, C., 2014. Some properties of the walls of metaxylem vessels of maize roots, including tests of the wettability of their lumenal wall surfaces. Annals of Botany 113, 977–989. https://doi.org/10.1093/aob/mcu020

McElrone, A.J., Grant, J.A., Kluepfel, D.A., 2010. The role of tyloses in crown hydraulic failure of mature walnut trees afflicted by apoplexy disorder. Tree Physiology 30, 761–772. https://doi.org/10.1093/treephys/tpq026

McElrone, A.J., Jackson, S., Habdas, P., 2008. Hydraulic disruption and passive migration by a bacterial pathogen in oak tree xylem. Journal of Experimental Botany 59, 2649–2657. https://doi.org/10.1093/jxb/ern124

Mirone, A., Gouillart, E., Brun, E., Tafforeau, P., Kieffer, J., 2014. PyHST2: an hybrid distributed code for high speed tomographic reconstruction with iterative

reconstruction and a priori knowledge capabilities. Nuclear Instruments and Methods in Physics Research Section B: Beam Interactions with Materials and Atoms 324, 41–48. https://doi.org/10.1016/j.nimb.2013.09.030

Mondello, V., Larignon, P., Armengol, J., Kortekamp, A., Vaczy, K., Prezman, F., Serrano, E., Rego, C., Mugnai, L., Fontaine, F., 2018. Management of grapevine trunk diseases: knowledge transfer, current strategies and innovative strategies adopted in Europe. Phytopathologia Mediterranea 57, 369–383. https://doi.org/10.14601/Phytopathol_Mediterr-23942

Morales-Cruz, A., Allenbeck, G., Figueroa-Balderas, R., Ashworth, V.E., Lawrence, D.P., Travadon, R., Smith, R.J., Baumgartner, K., Rolshausen, P.E., Cantu, D., 2018. Closed-reference metatranscriptomics enables *in planta* profiling of putative virulence activities in the grapevine trunk disease complex: Transcriptomics of pathogen communities. Molecular Plant Pathology 19, 490–503. https://doi.org/10.1111/mpp.12544

Mugnai, L., Graniti , A., Surico, G., 1999. Esca (Black measles) and brown wood streaking: two old and elusive diseases of grapevines. Plant Disease 83, 404-417. http://dx.doi.org/10.1094/PDIS.1999.83.5.404

Neghliz, H., Cochard, H., Brunel, N., Martre, P., 2016. Ear rachis xylem occlusion and associated loss in hydraulic conductance coincide with the end of grain filling for wheat. Frontiers in Plant Science 7, 920. https://doi.org/10.3389/fpls.2016.00920

Newbanks, D., 1983. Evidence for xylem dysfunction by embolization in dutch elm disease. Phytopathology 73, 1060. https://doi.org/10.1094/Phyto-73-1060

Oliva, J., Stenlid, J., Martínez-Vilalta, J., 2014. The effect of fungal pathogens on the water and carbon economy of trees: implications for drought-induced mortality. New Phytologist 203, 1028–1035. https://doi.org/10.1111/nph.12857

Oses, R., Valenzuela, S., Freer, J., Sanfuentes, E., Rodriguez, J., 2008. Fungal endophytes in xylem of healthy Chilean trees and their possible role in early wood decay. Fungal diversity 33, 77–86.

Paganin, D., Mayo, S.C., Gureyev, T.E., Miller, P.R., Wilkins, S.W., 2002. Simultaneous phase and amplitude extraction from a single defocused image of a homogeneous object. Journal of Microscopy 206, 33–40. https://doi.org/10.1046/j.1365-2818.2002.01010.x

Parke, J.L., Oh, E., Voelker, S., Hansen, E.M., Buckles, G., Lachenbruch, B., 2007. *Phytophthora ramorum* colonizes tanoak xylem and is associated with reduced stem water transport. Phytopathology 97, 1558–1567. https://doi.org/10.1094/PHYTO-97-12-1558

Pearce, R.B., 1996. Antimicrobial defences in the wood of living trees. New Phytologist 132, 203–233. https://doi.org/10.1111/j.1469-8137.1996.tb01842.x

Perez-Donoso, A.G., Greve, L.C., Walton, J.H., Shackel, K.A., Labavitch, J.M., 2006. *Xylella fastidiosa* infection and ethylene exposure result in xylem and water movement disruption in grapevine shoots. Plant Physiology 143, 1024–1036. https://doi.org/10.1104/pp.106.087023

Pérez-Donoso, A.G., Lenhof, J.J., Pinney, K., Labavitch, J.M., 2016. Vessel embolism and tyloses in early stages of Pierce's disease. Australian Journal of Grape and Wine Research 22, 81–86. https://doi.org/10.1111/ajgw.12178

Petit, A.-N., Vaillant, N., Boulay, M., Clément, C., Fontaine, F., 2006. Alteration of photosynthesis in grapevines affected by esca. Phytopathology 96, 1060–1066. https://doi.org/10.1094/PHYTO-96-1060

Pouzoulet, J., Mailhac, N., Couderc, C., Besson, X., Daydé, J., Lummerzheim, M., Jacques, A., 2013. A method to detect and quantify *Phaeomoniella chlamydospora* and *Phaeoacremonium aleophilum* DNA in grapevine-wood samples. Applied microbiology and biotechnology 97, 10163-10175. https://doi.org/10.1007/s00253-013-5299-6

Pouzoulet, J., Pivovaroff, A.L., Santiago, L.S., Rolshausen, P.E., 2014. Can vessel dimension explain tolerance toward fungal vascular wilt diseases in woody plants? Lessons from Dutch elm disease and esca disease in grapevine. Frontiers in Plant Science 5. https://doi.org/10.3389/fpls.2014.00253

Pouzoulet, J., Scudiero, E., Schiavon, M., Rolshausen, P.E., 2017. Xylem Vessel Diameter Affects the Compartmentalization of the Vascular Pathogen *Phaeomoniella chlamydospora* in Grapevine. Frontiers in Plant Science 8. https://doi.org/10.3389/fpls.2017.01442

Pratt, R. B., Jacobsen, A. L., 2018. Identifying which conduits are moving water in woody plants: a new HRCT-based method. Tree physiology 38, 1200-1212. https://doi.org/10.1093/treephys/tpy034

Qi, F., Jing, T., Zhan, Y., 2012. Characterization of endophytic fungi from *Acer ginnala* Maxim. in an artificial plantation: media effect and tissue-dependent variation. PLoS ONE 7, e46785. https://doi.org/10.1371/journal.pone.0046785

Reis, P., Pierron, R., Larignon, P., Lecomte, P., Abou-Mansour, E., Farine, S., Bertsch, C., Jacques, A., Trotel-Aziz, P., Rego, C. and Fontaine, F. 2019. Vitis Methods to Understand and Develop Strategies for Diagnosis and Sustainable Control of Grapevine Trunk Diseases. Phytopathology 109, pp.916-931. https://doi.org/10.1094/PHYTO-09-18-0349-RVW

Rioux, D., Nicole, M., Simard, M., Ouellette, G.B., 1998. Immunocytochemical evidence that secretion of pectin occurs during gel (gum) and tylosis formation in trees. Phytopathology 88, 494–505. https://doi.org/10.1094/PHYTO.1998.88.6.494

Salleo, S., Nardini, A., Lo Gullo, M.A., Ghirardelli, L.A., 2002. Changes in stem and leaf hydraulics preceding leaf shedding in *Castanea sativa* L. Biologia plantarum 45, 227–234. https://doi.org/10.1023/A:1015192522354

Sun, Q., Rost, T.L., Reid, M.S., Matthews, M.A., 2007. Ethylene and not embolism is required for wound-induced tylose development in stems of grapevines. Plant Physiology 145, 1629–1636. https://doi.org/10.1104/pp.107.100537

Sun, Q., Rost, T.L., Matthews, M.A., 2008. Wound-induced vascular occlusions in Vitis vinifera (Vitaceae): Tyloses in summer and gels in winter1. American Journal of Botany 95, 1498–1505. https://doi.org/10.3732/ajb.0800061

Sun, Q., Sun, Y., Walker, M.A., Labavitch, J.M., 2013. Vascular occlusions in grapevines with Pierce's disease make disease symptom development worse. Plant Physiology 161, 1529–1541. https://doi.org/10.1104/pp.112.208157

Surico, G., Mugnai, L., Marchi, G., 2006. Older and more recent observations on esca: a critical overview. Phytopathologia Mediterranea 45, S68–S86. http://dx.doi.org/10.14601/Phytopathol_Mediterr-1847

Surico, G., 2009. Towards a redefinition of the diseases within the esca complex of grapevine. Phytopathologia Mediterranea 48, 05–10. http://dx.doi.org/10.14601/Phytopathol_Mediterr-2870

Torres-Ruiz, J.M., Jansen, S., Choat, B., McElrone, A.J., Cochard, H., Brodribb, T.J., Badel, E., Burlett, R., Bouche, P.S., Brodersen, C.R., Li, S., Morris, H., Delzon, S., 2015. Direct X-Ray microtomography observation confirms the induction of embolism upon xylem cutting under tension. Plant Physiology 167, 40–43. https://doi.org/10.1104/pp.114.249706

Umebayashi, T., Fukuda, K., Haishi, T., Sotooka, R., Zuhair, S., Otsuki, K., 2011. The developmental process of xylem embolisms in pine wilt disease monitored by multipoint imaging using compact magnetic resonance imaging. Plant Physiology 156, 943–951. https://doi.org/10.1104/pp.110.170282

Valtaud, C., Foyer, C.H., Fleurat-Lessard, P., Bourbouloux, A., 2009. Systemic effects on leaf glutathione metabolism and defence protein expression caused by esca infection in grapevines. Functional Plant Biology 36, 260. https://doi.org/10.1071/FP08293

Valtaud, C., Thibault, F., Larignon, P., Bertsch, C., Fleurat-Lessard, P., Bourbouloux, A., 2011. Systemic damage in leaf metabolism caused by esca infection in grapevines: Starch and soluble sugars in esca-infected *Vitis* leaves. Australian Journal of Grape and Wine Research 17, 101–110. https://doi.org/10.1111/j.1755-0238.2010.00122.x

White, C., Hallen, F., Mostert, L., 2011. Symptoms and fungi associated with esca in South African vineyards. Phytopathologia Mediterranea 50, 236–246. http://dx.doi.org/10.14601/Phytopathol_Mediterr-8982

Yadeta, K.A., J. Thomma, B.P.H., 2013. The xylem as battleground for plant hosts and vascular wilt pathogens. Frontiers in Plant Science 4. https://doi.org/10.3389/fpls.2013.00097

Zimmermann, M.H., 1978. Vessel ends and the disruption of water flow in plants. The American Phytopathological Society.

Zimmermann, M.H., 1979. The Discovery of Tylose Formation by a Viennese lady in 1845. IAWA Bulletin 51–56.

Zimmermann, M.H., 1983. Xylem structure and the ascent of sap. Springer-Verlag, Berlin; New York.

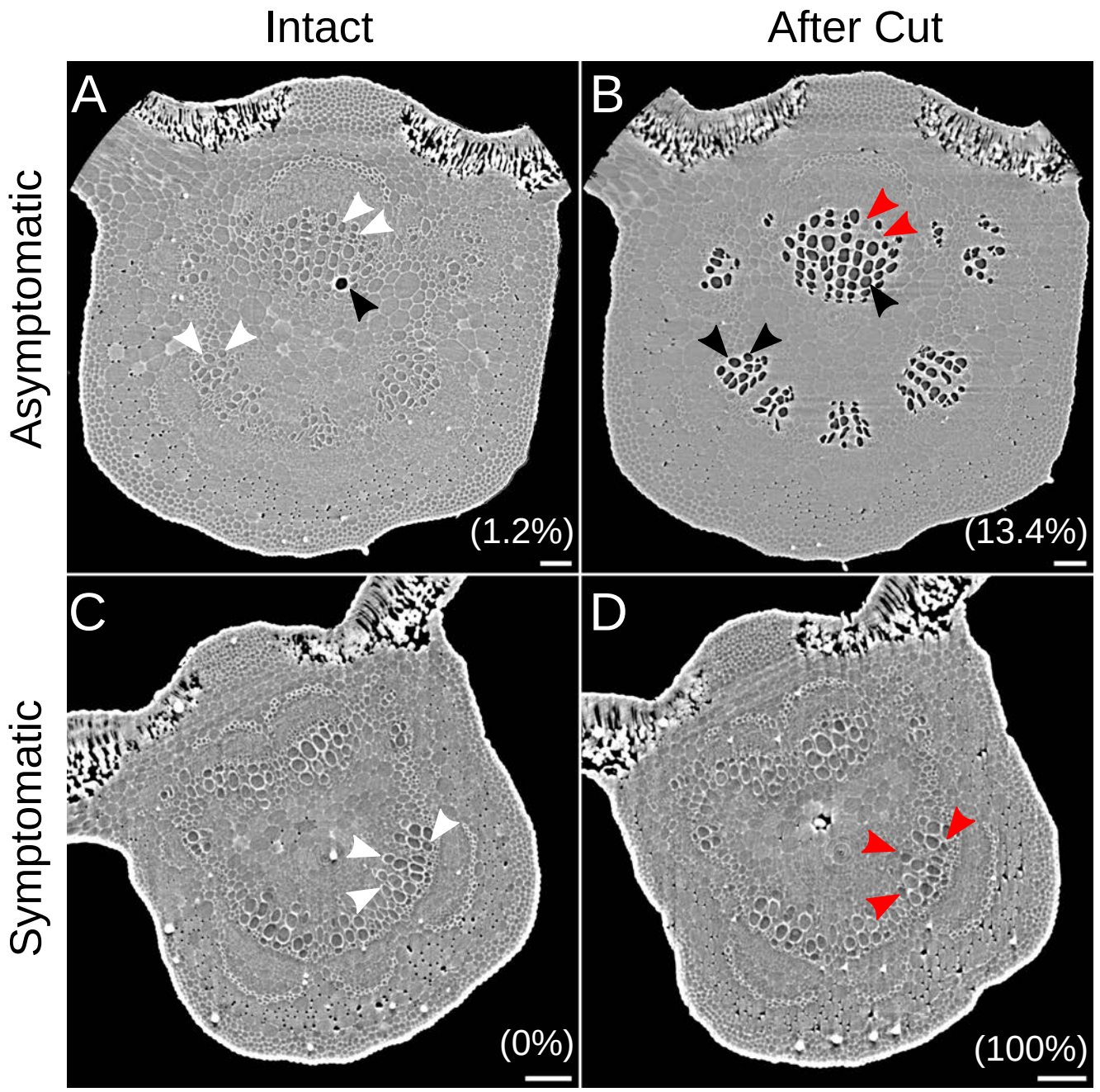

Figure 1. Two-dimensional reconstructions of cross sections from microCT volumes of *V. vinifera* leaves. Esca asymptomatic (**A**, **B**) and esca symptomatic (**C**, **D**) leaf midribs of *V. vinifera* plants. After a first scan on intact leaves (**A, C**) the samples were cut (**B, D**) just above the scanned area to embolize the vessels and then scanned again. Air-filled (*e.g.* black arrows), water-filled (*e.g.* white arrows), and occluded (*e.g.* red arrows) vessels were counted and their cross-sectional diameters quantified to determine the percentage loss of conductivity (PLC). The PLC represented by either native embolism (**A**, **C**) or occluded vessels (**B**, **D**) is given in parentheses. Scale bar = 100µm.

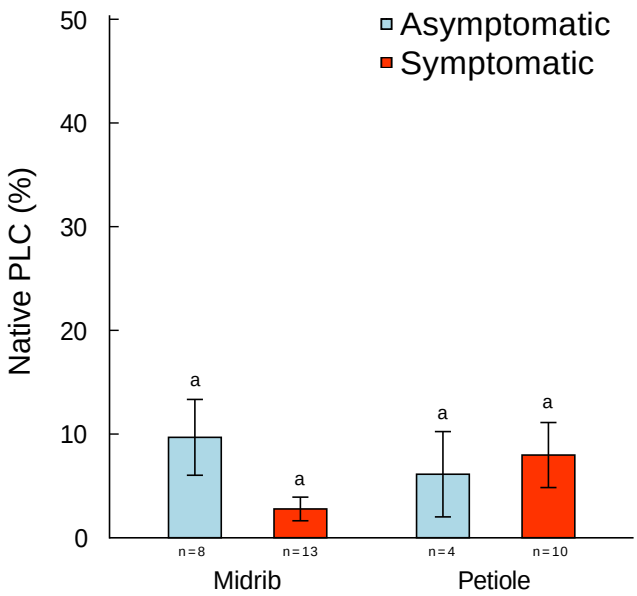

Figure 2. Mean native PLC in midribs and petioles of esca asymptomatic (blue) and esca symptomatic (red) leaves of *V. vinifera* plants using microCT imaging. PLC was calculated from the diameter of air-filled vessels in intact leaves, based on the total theoretical hydraulic conductivity of each sample. Error bars represent ± standard errors and different letters represent statistically significant differences (least squares means differences of fixed effects, *P*-value < 0.05, n=sample size).

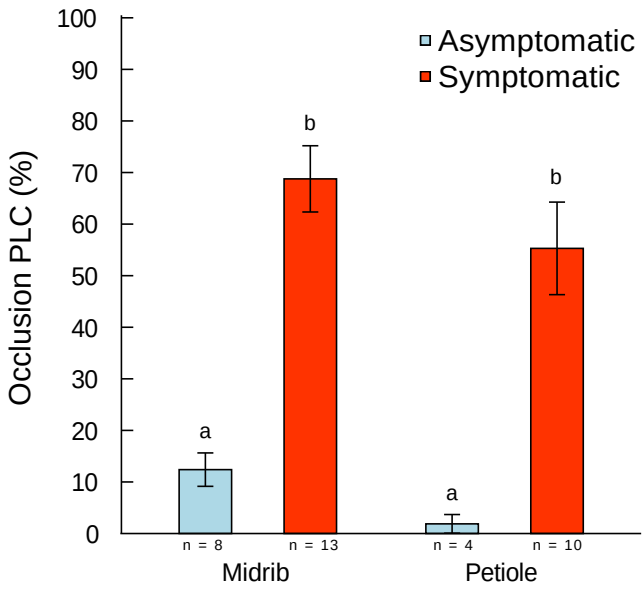

Figure 3. Mean occlusion PLC in midribs and petioles of esca asymptomatic (blue) and esca symptomatic (red) leaves of *V. vinifera* plants using microCT imaging. PLC was calculated from the diameter of occluded vessels, based on the total theoretical hydraulic conductivity of each sample. Error bars represent ± standard errors and different letters represent statistically significant differences (least squares means differences of fixed effects, *P*-value < 0.05, n=sample size).

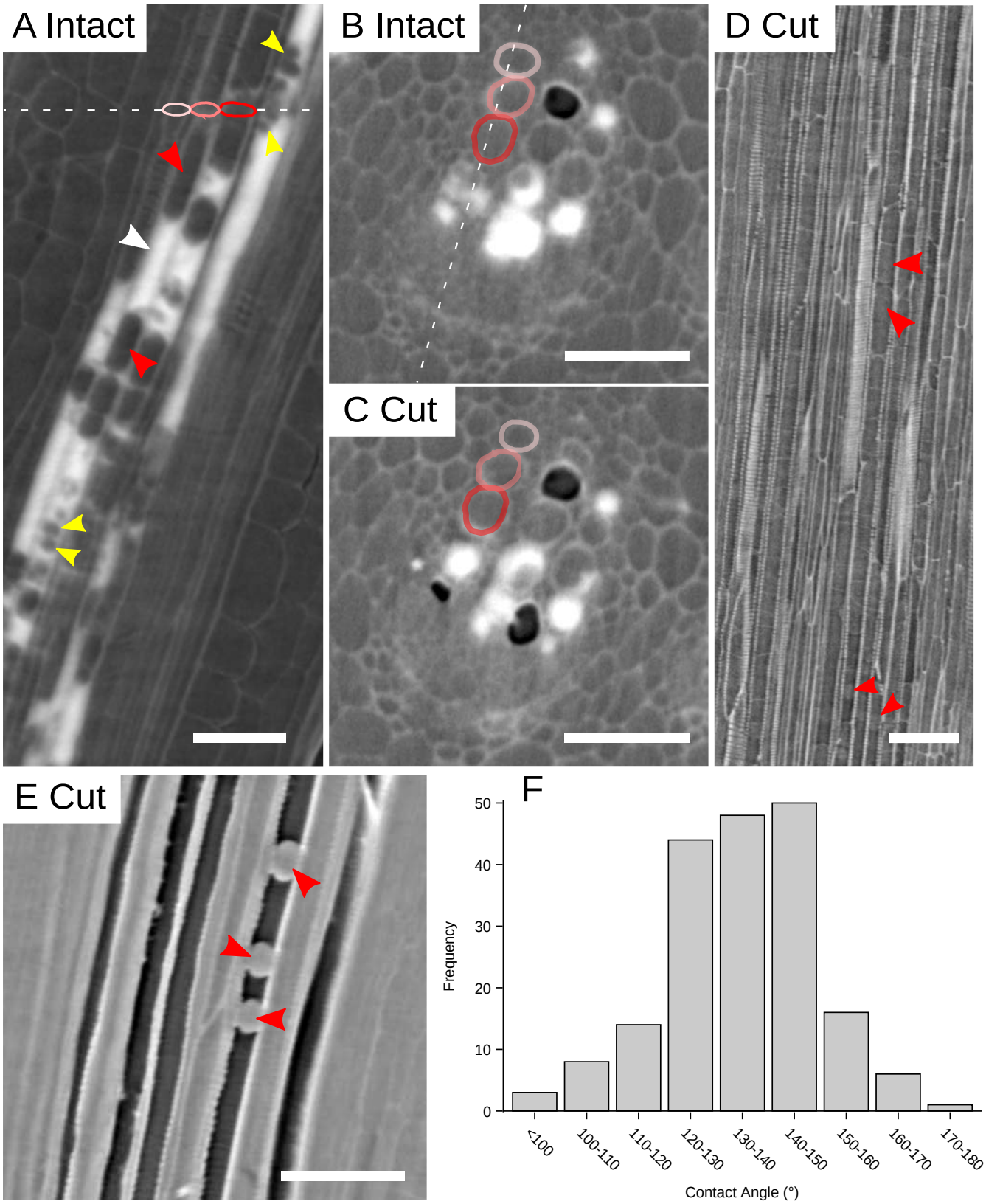

Figure 4. Two-dimensional reconstructions from microCT volumes of esca symptomatic leaves of *V. vinifera*. (**A-C**) Iohexol-fed midrib viewed in a longitudinal (**A**) and cross sections (**B**, **C**). For clarity and orientation the same three vessels are color coded and dotted lines represent the location of the sections relative to each other. The contrasting agent iohexol appears bright white and allows for the identification of the water transport pathway. The iohexol signal can even be seen in partially-occluded vessels (e.g. white arrow). Occlusions (i.e. gels or tyloses) can span the entire diameter of the vessel (red arrows) or only a portion (yellow arrows). After a first scan on intact leaves (**A, B**), the sample was cut (**C**) just above the scanned area and scanned again. (**D**) Longitudinal-section of a midrib with completely occluded vessels; the presence of occlusions are visible (although obscure) inside the vessel lumen (red arrows). (**E**) Longitudinal-section of an air-filled midrib (after cutting) with clearly visible occlusions (red arrows). (**F**) Frequency distribution of the contact angles between the occlusions and the vessel wall (sample size=190). Scale bars=100µm.

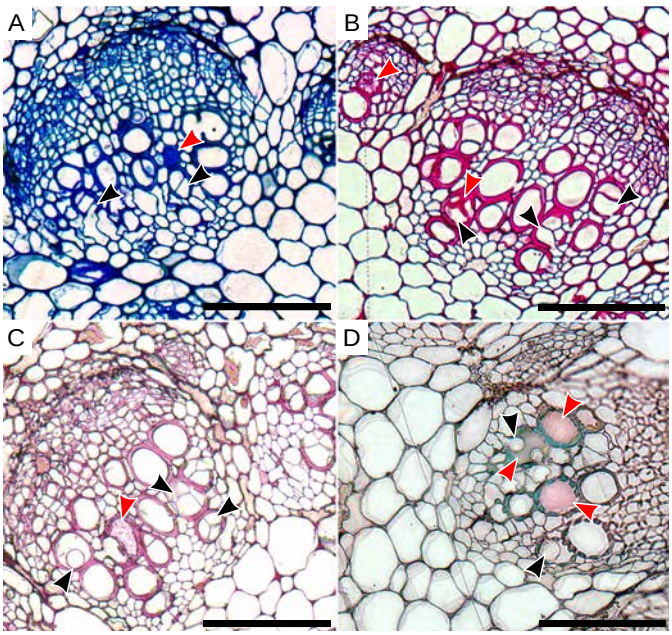

Figure 5. Light microscopy images of cross sections of esca symptomatic midribs of *V. vinifera*. Cross-sections were stained with toluidine blue O (**A**), periodic-acid Schiff's reactive (**B**), ruthenium red (**C**), and lacmoid blue (**D**). Red arrows indicate the presence of gels filling entirely the vessel lumen while black arrows indicate the presence of tyloses in vessel lumina. Scale bars = 100µm.

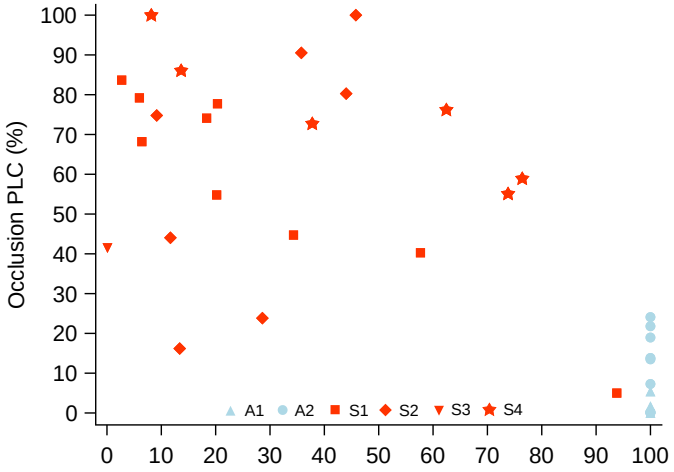

Figure 6. Relationship between the esca symptom severity (expressed as % green tissue per leaf) and the theoretical loss of hydraulic conductivity due to occluded vessels (occlusion PLC) in midribs and petioles of *V. vinifera*. Points are grouped by plant: A1, A2 (blue, asymptomatic), S1-S4 (red, symptomatic). The relationship between PLC and green tissue is not significant among symptomatic samples (red points, P-value=0.25).

Parsed Citations

Abou-Mansour, E., Couché, E., Tabacchi, R., 2004. Do fungal naphthalenones have a role in the development of esca symptoms? Phytopathologia Mediterranea 43, 75–82. http://dx.doi.org/10.14601/Phytopathol_Mediterr-1728

Pubmed: Author and Title
Google Scholar: Author Only Title Only Author and Title

Andolfi, A., Mugnai, L., Luque, J., Surico, G., Cimmino, A., Evidente, A., 2011. Phytotoxins produced by fungi associated with grapevine trunk diseases. Toxins 3, 1569–1605. https://doi.org/10.3390/toxins3121569

Pubmed: Author and Title
Google Scholar: Author Only Title Only Author and Title

Andreini, L., Caruso, G., Bertolla, C., Scalabrelli, G., Viti, R., Gucci, R., 2009. Gas exchange, stem water potential and xylem flux on some grapevine cultivars affected by esca disease. South African Journal of Enology & Viticulture 30. https://doi.org/10.21548/30-2-1434

Pubmed: Author and Title
Google Scholar: Author Only Title Only Author and Title

Beckman, C.H., Roberts, E.M., 1995. On the nature and genetic basis for resistance and tolerance to fungal wilt diseases of plants, in: Advances in Botanical Research. Elsevier, pp. 35–77. https://doi.org/10.1016/S0065-2296(08)60008-7

Pubmed: Author and Title
Google Scholar: Author Only Title Only Author and Title

Bertsch, C., Ramírez-Suero, M., Magnin-Robert, M., Larignon, P., Chong, J., Abou-Mansour, E., Spagnolo, A., Clément, C., Fontaine, F., 2013. Grapevine trunk diseases: complex and still poorly understood. Plant Pathology 62, 243–265. https://doi.org/10.1111/j.1365-3059.2012.02674.x

Pubmed: Author and Title
Google Scholar: Author Only Title Only Author and Title

Bonsen, K.J.M., Kučera, L.J., 1990. Vessel Occlusions in Plants: Morphological, Functional and Evolutionary Aspects. IAWA Journal 11, 393–399. https://doi.org/10.1163/22941932-90000528

Pubmed: Author and Title
Google Scholar: Author Only Title Only Author and Title

Brodribb, T.J., Holbrook, N.M., 2003. stomatal closure during leaf dehydration, correlation with other leaf physiological traits. Plant Physiology 132, 2166–2173. https://doi.org/10.1104/pp.103.023879

Pubmed: Author and Title
Google Scholar: Author Only Title Only Author and Title

Bruez, E., Baumgartner, K., Bastien, S., Travadon, R., Guérin-Dubrana, L., Rey, P. 2016. Various fungal communities colonise the functional wood tissues of old grapevines externally free from grapevine trunk disease symptoms. Australian journal of grape and wine research, 22: 288-295. https://doi.org/10.1111/ajgw.12209

Pubmed: Author and Title
Google Scholar: Author Only Title Only Author and Title

Bruez, E., Vallance, J., Gerbore, J., Lecomte, P., Da Costa, J.-P., Guerin-Dubrana, L., Rey, P., 2014. Analyses of the temporal dynamics of fungal communities colonizing the healthy wood tissues of esca leaf-symptomatic and asymptomatic vines. PLoS ONE 9, e95928. https://doi.org/10.1371/journal.pone.0095928

Pubmed: Author and Title
Google Scholar: Author Only Title Only Author and Title

Bruno, G., Sparapano, L., 2006. Effects of three esca-associated fungi on Vitis vinifera L.: III. Enzymes produced by the pathogens and their role in fungus-to-plant or in fungus-to-fungus interactions. Physiological and Molecular Plant Pathology 69, 182–194. https://doi.org/10.1016/j.pmpp.2007.04.006

Pubmed: Author and Title
Google Scholar: Author Only Title Only Author and Title

Bruno, G., Sparapano, L., Graniti, A., 2007. Effects of three esca-associated fungi on Vitis vinifera L.: IV. diffusion through the xylem of metabolites produced by two tracheiphilous fungi in the woody tissue of grapevine leads to esca-like symptoms on leaves and berries. Physiological and Molecular Plant Pathology 71, 106–124. https://doi.org/10.1016/j.pmpp.2007.12.004

Pubmed: Author and Title
Google Scholar: Author Only Title Only Author and Title

Canny, M., 1997. Tyloses and the maintenance of transpiration. Annals of Botany 80, 565–570. https://doi.org/10.1006/anbo.1997.0475

Pubmed: Author and Title
Google Scholar: Author Only Title Only Author and Title

Choat, B., Gambetta, G.A., Wada, H., Shackel, K.A., Matthews, M.A., 2009. The effects of Pierce's disease on leaf and petiole hydraulic conductance in Vitis vinifera cv. Chardonnay. Physiologia Plantarum 136, 384–394. https://doi.org/10.1111/j.1399-3054.2009.01231.x

Pubmed: Author and Title
Google Scholar: Author Only Title Only Author and Title

Clérivet, A., Déon, V., Alami, I., Lopez, F., Geiger, J.-P., Nicole, M., 2000. Tyloses and ggels associated with cellulose accumulation in vessels are responses of plane tree seedlings (Platanus × acerifolia) to the vascular fungus Ceratocystis fimbriata f. sp platani. Trees

15, 25–31. https://doi.org/10.1007/s004680000063
Pubmed: Author and Title
Google Scholar: Author Only Title Only Author and Title

Cloete, M., Mostert, L., Fischer, M., Halleen, F. 2015. Pathogenicity of South African Hymenochaetales taxa isolated from esca-infected grapevines. Phytopathologia Mediterranea 54, 368-379. https://doi.org/10.14601/Phytopathol_Mediterr-16237
Pubmed: Author and Title
Google Scholar: Author Only Title Only Author and Title

Collins, B.R., Parke, J.L., Lachenbruch, B., Hansen, E.M., 2009. The effects of Phytophthora ramorum infection on hydraulic conductivity and tylosis formation in tanoak sapwood. Canadian Journal of Forest Research 39, 1766–1776. https://doi.org/10.1139/X09-097
Pubmed: Author and Title
Google Scholar: Author Only Title Only Author and Title

Del Rio, J.A., Gonzalez, A., Fuster, M.D., Botia, J.M., Gomez, P., Frias, V., Ortuno, A., 2001. Tylose formation and changes in phenolic compounds of grape roots infected with Phaeomoniella chlamydospora and Phaeoacremonium species. Phytopathologia Mediterranea 40, S394–S399. http://dx.doi.org/10.14601/Phytopathol_Mediterr-1644
Pubmed: Author and Title
Google Scholar: Author Only Title Only Author and Title

De Micco, V., Balzano, A., Wheeler, E. A., & Baas, P. 2016. Tyloses and gums: a review of structure, function and occurrence of vessel occlusions. IAWA journal 37, 186-205. http://dx.doi.org/10.1163/22941932-20160130
Pubmed: Author and Title
Google Scholar: Author Only Title Only Author and Title

Feliciano, A. J., Eskalen, A., Gubler, W. D., 2004. Differential susceptibility of three grapevine cultivars to the Phaeoacremoium aleophilum and Phaeomoniella chlamydospora in California. Phytopathologia Mediterranea 43, 66-69. http://dx.doi.org/10.14601/Phytopathol_Mediterr-1727
Pubmed: Author and Title
Google Scholar: Author Only Title Only Author and Title

Fischer, M., 2006. Biodiversity and geographic distribution of basidiomycetes causing esca-associated white rot in grapevine: a worldwide perspective. Phytopathologia Mediterranea 45, S30-S42.http://dx.doi.org/10.14601/Phytopathol_Mediterr-1846
Pubmed: Author and Title
Google Scholar: Author Only Title Only Author and Title

Fischer, M., Peighami-Ashnaei, S. 2019. Grapevine, esca complex, and environment: the disease triangle. Phytopathologia Mediterranea 58, 17-37. http://dx.doi.org/10.14601/Phytopathol_Mediterr-25086
Pubmed: Author and Title
Google Scholar: Author Only Title Only Author and Title

Fisher, P.J., Petrini, O., Sutton, B.C., 1993. A comparative study of fungal endophytes in leaves, xylem and bark of Eucalyptus in Australia and England. Sydowia 45, 338–345.
Pubmed: Author and Title
Google Scholar: Author Only Title Only Author and Title

Fontaine, F., Pinto, C., Vallet, J., Clément, C., Gomes, A.C., Spagnolo, A., 2016. The effects of grapevine trunk diseases (GTDs) on vine physiology. European Journal of Plant Pathology 144, 707–721. https://doi.org/10.1007/s10658-015-0770-0
Pubmed: Author and Title
Google Scholar: Author Only Title Only Author and Title

Fradin, E. F., Thomma, B. P., 2006. Physiology and molecular aspects of Verticillium wilt diseases caused by V. dahliae and V. albo-atrum. Molecular plant pathology 7, 71-86. https://doi.org/10.1111/j.1364-3703.2006.00323.x
Pubmed: Author and Title
Google Scholar: Author Only Title Only Author and Title

Gambetta, G.A., Fei, J., Rost, T.L., Matthews, M.A., 2007. Leaf scorch symptoms are not correlated with bacterial populations during Pierce's disease. Journal of Experimental Botany 58, 4037–4046. https://doi.org/10.1093/jxb/erm260
Pubmed: Author and Title
Google Scholar: Author Only Title Only Author and Title

Gómez, P., Báidez, A.G., Ortuño, A., Del Río, J.A., 2016. Grapevine xylem response to fungi involved in trunk diseases: Grapevine vascular defence. Annals of Applied Biology 169, 116–124. https://doi.org/10.1111/aab.12285
Pubmed: Author and Title
Google Scholar: Author Only Title Only Author and Title

Guerin-Dubrana, L., Fontaine, F., Mugnai, L. 2019. Grapevine trunk disease in European and Mediterranean vineyards: occurrence, distribution and associated disease-affecting cultural factors. Phytopathologia Mediterranea 58, 49-71. https://doi.org/10.13128/Phytopathol_Mediterr-25153
Pubmed: Author and Title
Google Scholar: Author Only Title Only Author and Title

Gramaje, D., Úrbez-Torres, J.R., Sosnowski, M.R., 2018. Managing grapevine trunk diseases with respect to etiology and epidemiology:

current strategies and future prospects. Plant Disease 102, 12–39. https://doi.org/10.1094/PDIS-04-17-0512-FE
Pubmed: Author and Title
Google Scholar: Author Only Title Only Author and Title

Hochberg, U., Windt, C.W., Ponomarenko, A., Zhang, Y-J., Gersony, J., et al. 2017. Stomatal closure, basal leaf embolism and shedding protect the hydraulic integrity of grape stems. Plant Physiologist, 174: 764–75. https://doi.org/10.1104/pp.16.01816
Pubmed: Author and Title
Google Scholar: Author Only Title Only Author and Title

Häffner, E., Konietzki, S., Diederichsen, E., 2015. Keeping control: the role of senescence and development in plant pathogenesis and defense. Plants 4, 449–488. https://doi.org/10.3390/plants4030449
Pubmed: Author and Title
Google Scholar: Author Only Title Only Author and Title

King, A., Guignot, N., Zerbino, P., Boulard, E., Desjardins, K., Bordessoule, M., Leclerq, N., Le, S., Renaud, G., Cerato, M., Bornert, M., Lenoir, N., Delzon, S., Perrillat, J.-P., Legodec, Y., Itié, J.-P., 2016. Tomography and imaging at the PSICHE beam line of the SOLEIL synchrotron. Review of Scientific Instruments 87, 093704. https://doi.org/10.1063/1.4961365
Pubmed: Author and Title
Google Scholar: Author Only Title Only Author and Title

Knipfer, T., Fei, J., Gambetta, G. A., McElrone, A. J., Shackel, K. A., Matthews, M. A. 2015. Water transport properties of the grape pedicel during fruit development: insights into xylem anatomy and function using microtomography. Plant Physiology 168, 1590-1602. https://doi.org/10.1104/pp.15.00031
Pubmed: Author and Title
Google Scholar: Author Only Title Only Author and Title

Kuroda, K., 2012. Monitoring of xylem embolism and dysfunction by the acoustic emission technique in Pinus thunbergii inoculated with the pine wood nematode Bursaphelenchus xylophilus. Journal of Forest Research 17, 58–64. https://doi.org/10.1007/s10310-010-0246-1
Pubmed: Author and Title
Google Scholar: Author Only Title Only Author and Title

Larignon, P. and Dubos, B., 1997. Fungi associated with esca disease in grapevine. European Journal of Plant Pathology 10, 147-157. https://doi.org/10.1023/A:1008638409410
Pubmed: Author and Title
Google Scholar: Author Only Title Only Author and Title

Lecomte, P., Darrieutort, G., Liminana, J. M., Comont, G., Muruamendiaraz, A., Legorburu, F. J., Choueiri, E., Jreijiri, F., El Amil, R., Fermaud, M., 2012. New insights into esca of grapevine: the development of foliar symptoms and their association with xylem discoloration. Plant Disease 96, 924-934. https://doi.org/10.1094/PDIS-09-11-0776-RE
Pubmed: Author and Title
Google Scholar: Author Only Title Only Author and Title

Lee, E.F., Matthews, M.A., McElrone, A.J., Phillips, R.J., Shackel, K.A., Brodersen, C.R., 2013. Analysis of HRCT-derived xylem network reveals reverse flow in some vessels. Journal of Theoretical Biology 333, 146–155. https://doi.org/10.1016/j.jtbi.2013.05.021
Pubmed: Author and Title
Google Scholar: Author Only Title Only Author and Title

Letousey, P., Baillieul, F., Perrot, G., Rabenoelina, F., Boulay, M., Vaillant-Gaveau, N., Clément, C., Fontaine, F., 2010. Early events prior to visual symptoms in the apoplectic form of grapevine esca disease. Phytopathology 100, 424-431.
Pubmed: Author and Title
Google Scholar: Author Only Title Only Author and Title

https://doi.org/10.1094/PHYTO-100-5-0424
Pubmed: Author and Title
Google Scholar: Author Only Title Only Author and Title

Luini, E., Fleurat-Lessard, P., Rousseau, L., Roblin, G., Berjeaud, J.-M., 2010. Inhibitory effects of polypeptides secreted by the grapevine pathogens Phaeomoniella chlamydospora and Phaeoacremonium aleophilum on plant cell activities. Physiological and Molecular Plant Pathology 74, 403–411. https://doi.org/10.1016/j.pmpp.2010.06.007
Pubmed: Author and Title
Google Scholar: Author Only Title Only Author and Title

Magnin-Robert, M., Letousey, P., Spagnolo, A., Rabenoelina, F., Jacquens, L., Mercier, L., Clément, C., Fontaine, F., 2011. Leaf stripe form of esca induces alteration of photosynthesis and defence reactions in presymptomatic leaves. Functional Plant Biology 38. https://doi.org/10.1071/FP11083
Pubmed: Author and Title
Google Scholar: Author Only Title Only Author and Title

Magnin-Robert, M., Spagnolo, A., Boulanger, A., Joyeux, C., Clément, C., Abou-Mansour, E., Fontaine, F., 2016. Changes in plant metabolism and accumulation of fungal metabolites in response to esca proper and apoplexy expression in the whole grapevine. Phytopathology 106, 541–553. https://doi.org/10.1094/PHYTO-09-15-0207-R
Pubmed: Author and Title
Google Scholar: Author Only Title Only Author and Title

Martín, L., Fontaine, F., Castaño, F.J., Songy, A., Roda, R., Vallet, J., Ferrer-Gallego, R., 2019. Specific profile of Tempranillo grapevines related to Esca-leaf symptoms and climate conditions. Plant Physiology and Biochemistry 135, 575–587. https://doi.org/10.1016/j.plaphy.2018.10.040
Pubmed: Author and Title
Google Scholar: Author Only Title Only Author and Title

Martin, N., Vesentini, D., Rego, C., Monteiro, S., Oliveira, H., Ferreira, R.B., 2009. Phaeomoniella chlamydospora infection induces changes in phenolic compounds content in Vitis vinifera. Phytopathologia Mediterranea 48, 101–116.
Pubmed: Author and Title
Google Scholar: Author Only Title Only Author and Title

http://dx.doi.org/10.14601/Phytopathol_Mediterr-2879
Pubmed: Author and Title
Google Scholar: Author Only Title Only Author and Title

Masi, M., Cimmino, A., Reveglia, P., Mugnai, L., Surico, G. and Evidente, A. 2018. Advances on fungal phytotoxins and their role in grapevine trunk diseases. Journal of agricultural and food chemistry 66, 5948-5958. https://doi.org/10.1021/acs.jafc.8b00773
Pubmed: Author and Title
Google Scholar: Author Only Title Only Author and Title

Massonnet., M., Morales-Cruz, A., Minio A., Figueroa-Balderas, R., Lawrence, D.P., Travadon, R., Rolshausen, P.E., Baumgartner, K., Cantu, D., 2018. Whole-genome resequencing and pan-transcriptome reconstruction highlight the impact of genomic structural variation on secondary metabolite gene clusters in the grapevine esca pathogen Phaeoacremonium minimum. Frontiers in Microbiology 9, 1784. https://doi.org/10.3389/fmicb.2018.01784
Pubmed: Author and Title
Google Scholar: Author Only Title Only Author and Title

McCully, M., Canny, M., Baker, A., Miller, C., 2014. Some properties of the walls of metaxylem vessels of maize roots, including tests of the wettability of their lumenal wall surfaces. Annals of Botany 113, 977–989. https://doi.org/10.1093/aob/mcu020
Pubmed: Author and Title
Google Scholar: Author Only Title Only Author and Title

McElrone, A.J., Grant, J.A., Kluepfel, D.A., 2010. The role of tyloses in crown hydraulic failure of mature walnut trees afflicted by apoplexy disorder. Tree Physiology 30, 761–772. https://doi.org/10.1093/treephys/tpq026
Pubmed: Author and Title
Google Scholar: Author Only Title Only Author and Title

McElrone, A.J., Jackson, S., Habdas, P., 2008. Hydraulic disruption and passive migration by a bacterial pathogen in oak tree xylem. Journal of Experimental Botany 59, 2649–2657. https://doi.org/10.1093/jxb/ern124
Pubmed: Author and Title
Google Scholar: Author Only Title Only Author and Title

Mirone, A., Gouillart, E., Brun, E., Tafforeau, P., Kieffer, J., 2014. PyHST2: an hybrid distributed code for high speed tomographic reconstruction with iterative reconstruction and a priori knowledge capabilities. Nuclear Instruments and Methods in Physics Research Section B: Beam Interactions with Materials and Atoms 324, 41–48. https://doi.org/10.1016/j.nimb.2013.09.030
Pubmed: Author and Title
Google Scholar: Author Only Title Only Author and Title

Mondello, V., Larignon, P., Armengol, J., Kortekamp, A., Vaczy, K., Prezman, F., Serrano, E., Rego, C., Mugnai, L., Fontaine, F., 2018. Management of grapevine trunk diseases: knowledge transfer, current strategies and innovative strategies adopted in Europe. Phytopathologia Mediterranea 57, 369–383. https://doi.org/10.14601/Phytopathol_Mediterr-23942
Pubmed: Author and Title
Google Scholar: Author Only Title Only Author and Title

Morales-Cruz, A., Allenbeck, G., Figueroa-Balderas, R., Ashworth, V.E., Lawrence, D.P., Travadon, R., Smith, R.J., Baumgartner, K., Rolshausen, P.E., Cantu, D., 2018. Closed-reference metatranscriptomics enables in planta profiling of putative virulence activities in the grapevine trunk disease complex: Transcriptomics of pathogen communities. Molecular Plant Pathology 19, 490–503. https://doi.org/10.1111/mpp.12544
Pubmed: Author and Title
Google Scholar: Author Only Title Only Author and Title

Mugnai, L., Graniti , A., Surico, G., 1999. Esca (Black measles) and brown wood streaking: two old and elusive diseases of grapevines. Plant Disease 83, 404-417. http://dx.doi.org/10.1094/PDIS.1999.83.5.404
Pubmed: Author and Title
Google Scholar: Author Only Title Only Author and Title

Neghliz, H., Cochard, H., Brunel, N., Martre, P., 2016. Ear rachis xylem occlusion and associated loss in hydraulic conductance coincide with the end of grain filling for wheat. Frontiers in Plant Science 7, 920. https://doi.org/10.3389/fpls.2016.00920
Pubmed: Author and Title
Google Scholar: Author Only Title Only Author and Title

Newbanks, D., 1983. Evidence for xylem dysfunction by embolization in dutch elm disease. Phytopathology 73, 1060. https://doi.org/10.1094/Phyto-73-1060
Pubmed: Author and Title

Google Scholar: Author Only Title Only Author and Title

Oliva, J., Stenlid, J., Martínez-Vilalta, J., 2014. The effect of fungal pathogens on the water and carbon economy of trees: implications for drought-induced mortality. New Phytologist 203, 1028–1035. https://doi.org/10.1111/nph.12857
Pubmed: Author and Title
Google Scholar: Author Only Title Only Author and Title

Oses, R., Valenzuela, S., Freer, J., Sanfuentes, E., Rodriguez, J., 2008. Fungal endophytes in xylem of healthy Chilean trees and their possible role in early wood decay. Fungal diversity 33, 77–86.
Pubmed: Author and Title
Google Scholar: Author Only Title Only Author and Title

Paganin, D., Mayo, S.C., Gureyev, T.E., Miller, P.R., Wilkins, S.W., 2002. Simultaneous phase and amplitude extraction from a single defocused image of a homogeneous object. Journal of Microscopy 206, 33–40. https://doi.org/10.1046/j.1365-2818.2002.01010.x
Pubmed: Author and Title
Google Scholar: Author Only Title Only Author and Title

Parke, J.L., Oh, E., Voelker, S., Hansen, E.M., Buckles, G., Lachenbruch, B., 2007. Phytophthora ramorum colonizes tanoak xylem and is associated with reduced stem water transport. Phytopathology 97, 1558–1567. https://doi.org/10.1094/PHYTO-97-12-1558
Pubmed: Author and Title
Google Scholar: Author Only Title Only Author and Title

Pearce, R.B., 1996. Antimicrobial defences in the wood of living trees. New Phytologist 132, 203–233. https://doi.org/10.1111/j.1469-8137.1996.tb01842.x
Pubmed: Author and Title
Google Scholar: Author Only Title Only Author and Title

Perez-Donoso, A.G., Greve, L.C., Walton, J.H., Shackel, K.A., Labavitch, J.M., 2006. Xylella fastidiosa infection and ethylene exposure result in xylem and water movement disruption in grapevine shoots. Plant Physiology 143, 1024–1036. https://doi.org/10.1104/pp.106.087023
Pubmed: Author and Title
Google Scholar: Author Only Title Only Author and Title

Pérez-Donoso, A.G., Lenhof, J.J., Pinney, K., Labavitch, J.M., 2016. Vessel embolism and tyloses in early stages of Pierce's disease. Australian Journal of Grape and Wine Research 22, 81–86. https://doi.org/10.1111/ajgw.12178
Pubmed: Author and Title
Google Scholar: Author Only Title Only Author and Title

Petit, A.-N., Vaillant, N., Boulay, M., Clément, C., Fontaine, F., 2006. Alteration of photosynthesis in grapevines affected by esca. Phytopathology 96, 1060–1066. https://doi.org/10.1094/PHYTO-96-1060
Pubmed: Author and Title
Google Scholar: Author Only Title Only Author and Title

Pouzoulet, J., Mailhac, N., Couderc, C., Besson, X., Daydé, J., Lummerzheim, M., Jacques, A., 2013. A method to detect and quantify Phaeomoniella chlamydospora and Phaeoacremonium aleophilum DNA in grapevine-wood samples. Applied microbiology and biotechnology 97, 10163-10175. https://doi.org/10.1007/s00253-013-5299-6
Pubmed: Author and Title
Google Scholar: Author Only Title Only Author and Title

Pouzoulet, J., Pivovaroff, A.L., Santiago, L.S., Rolshausen, P.E., 2014. Can vessel dimension explain tolerance toward fungal vascular wilt diseases in woody plants? Lessons from Dutch elm disease and esca disease in grapevine. Frontiers in Plant Science 5. https://doi.org/10.3389/fpls.2014.00253
Pubmed: Author and Title
Google Scholar: Author Only Title Only Author and Title

Pouzoulet, J., Scudiero, E., Schiavon, M., Rolshausen, P.E., 2017. Xylem Vessel Diameter Affects the Compartmentalization of the Vascular Pathogen Phaeomoniella chlamydospora in Grapevine. Frontiers in Plant Science 8. https://doi.org/10.3389/fpls.2017.01442
Pubmed: Author and Title
Google Scholar: Author Only Title Only Author and Title

Pratt, R. B., Jacobsen, A. L., 2018. Identifying which conduits are moving water in woody plants: a new HRCT-based method. Tree physiology 38, 1200-1212. https://doi.org/10.1093/treephys/tpy034
Pubmed: Author and Title
Google Scholar: Author Only Title Only Author and Title

Qi, F., Jing, T., Zhan, Y., 2012. Characterization of endophytic fungi from Acer ginnala Maxim. in an artificial plantation: media effect and tissue-dependent variation. PLoS ONE 7, e46785. https://doi.org/10.1371/journal.pone.0046785
Pubmed: Author and Title
Google Scholar: Author Only Title Only Author and Title

Reis, P., Pierron, R., Larignon, P., Lecomte, P., Abou-Mansour, E., Farine, S., Bertsch, C., Jacques, A., Trotel-Aziz, P., Rego, C. and Fontaine, F. 2019. Vitis Methods to Understand and Develop Strategies for Diagnosis and Sustainable Control of Grapevine Trunk Diseases. Phytopathology 109, pp.916-931. https://doi.org/10.1094/PHYTO-09-18-0349-RVW
Pubmed: Author and Title
Google Scholar: Author Only Title Only Author and Title

Rioux, D., Nicole, M., Simard, M., Ouellette, G.B., 1998. Immunocytochemical evidence that secretion of pectin occurs during gel (gum) and tylosis formation in trees. Phytopathology 88, 494–505. https://doi.org/10.1094/PHYTO.1998.88.6.494
Pubmed: Author and Title
Google Scholar: Author Only Title Only Author and Title

Salleo, S., Nardini, A., Lo Gullo, M.A., Ghirardelli, L.A., 2002. Changes in stem and leaf hydraulics preceding leaf shedding in Castanea sativa L. Biologia plantarum 45, 227–234. https://doi.org/10.1023/A:1015192522354
Pubmed: Author and Title
Google Scholar: Author Only Title Only Author and Title

Sun, Q., Rost, T.L., Reid, M.S., Matthews, M.A., 2007. Ethylene and not embolism is required for wound-induced tylose development in stems of grapevines. Plant Physiology 145, 1629–1636. https://doi.org/10.1104/pp.107.100537
Pubmed: Author and Title
Google Scholar: Author Only Title Only Author and Title

Sun, Q., Rost, T.L., Matthews, M.A., 2008. Wound-induced vascular occlusions in Vitis vinifera (Vitaceae): Tyloses in summer and gels in winter1. American Journal of Botany 95, 1498–1505. https://doi.org/10.3732/ajb.0800061
Pubmed: Author and Title
Google Scholar: Author Only Title Only Author and Title

Sun, Q., Sun, Y., Walker, M.A., Labavitch, J.M., 2013. Vascular occlusions in grapevines with Pierce's disease make disease symptom development worse. Plant Physiology 161, 1529–1541. https://doi.org/10.1104/pp.112.208157
Pubmed: Author and Title
Google Scholar: Author Only Title Only Author and Title

Surico, G., Mugnai, L., Marchi, G., 2006. Older and more recent observations on esca: a critical overview. Phytopathologia Mediterranea 45, S68–S86. http://dx.doi.org/10.14601/Phytopathol_Mediterr-1847
Pubmed: Author and Title
Google Scholar: Author Only Title Only Author and Title

Surico, G., 2009. Towards a redefinition of the diseases within the esca complex of grapevine. Phytopathologia Mediterranea 48, 05–10. http://dx.doi.org/10.14601/Phytopathol_Mediterr-2870
Pubmed: Author and Title
Google Scholar: Author Only Title Only Author and Title

Torres-Ruiz, J.M., Jansen, S., Choat, B., McElrone, A.J., Cochard, H., Brodribb, T.J., Badel, E., Burlett, R., Bouche, P.S., Brodersen, C.R., Li, S., Morris, H., Delzon, S., 2015. Direct X-Ray microtomography observation confirms the induction of embolism upon xylem cutting under tension. Plant Physiology 167, 40–43. https://doi.org/10.1104/pp.114.249706
Pubmed: Author and Title
Google Scholar: Author Only Title Only Author and Title

Umebayashi, T., Fukuda, K., Haishi, T., Sotooka, R., Zuhair, S., Otsuki, K., 2011. The developmental process of xylem embolisms in pine wilt disease monitored by multipoint imaging using compact magnetic resonance imaging. Plant Physiology 156, 943–951. https://doi.org/10.1104/pp.110.170282
Pubmed: Author and Title
Google Scholar: Author Only Title Only Author and Title

Valtaud, C., Foyer, C.H., Fleurat-Lessard, P., Bourbouloux, A., 2009. Systemic effects on leaf glutathione metabolism and defence protein expression caused by esca infection in grapevines. Functional Plant Biology 36, 260. https://doi.org/10.1071/FP08293
Pubmed: Author and Title
Google Scholar: Author Only Title Only Author and Title

Valtaud, C., Thibault, F., Larignon, P., Bertsch, C., Fleurat-Lessard, P., Bourbouloux, A., 2011. Systemic damage in leaf metabolism caused by esca infection in grapevines: Starch and soluble sugars in esca-infected Vitis leaves. Australian Journal of Grape and Wine Research 17, 101–110. https://doi.org/10.1111/j.1755-0238.2010.00122.x
Pubmed: Author and Title
Google Scholar: Author Only Title Only Author and Title

White, C., Hallen, F., Mostert, L., 2011. Symptoms and fungi associated with esca in South African vineyards. Phytopathologia Mediterranea 50, 236–246. http://dx.doi.org/10.14601/Phytopathol_Mediterr-8982
Pubmed: Author and Title
Google Scholar: Author Only Title Only Author and Title

Yadeta, K.A., J. Thomma, B.P.H., 2013. The xylem as battleground for plant hosts and vascular wilt pathogens. Frontiers in Plant Science 4. https://doi.org/10.3389/fpls.2013.00097
Pubmed: Author and Title
Google Scholar: Author Only Title Only Author and Title

Zimmermann, M.H., 1978. Vessel ends and the disruption of water flow in plants. The American Phytopathological Society.
Pubmed: Author and Title
Google Scholar: Author Only Title Only Author and Title

Zimmermann, M.H., 1979. The Discovery of Tylose Formation by a Viennese lady in 1845. IAWA Bulletin 51–56.

Pubmed: Author and Title
Google Scholar: Author Only Title Only Author and Title

Zimmermann, M.H., 1983. Xylem structure and the ascent of sap. Springer-Verlag, Berlin; New York.
Pubmed: Author and Title
Google Scholar: Author Only Title Only Author and Title